Elevated *Plasmodium falciparum* sexual conversion in HbAC and HbAS red blood cells in naturally infected malaria patients

Yasmina Drissi-El Boukili[1,3], Vera Kühne[1], H. Magloire Natama[4], Pieter Moris[1], Elisabet Tintó-Font[6], Odin Goovaerts[2], Pieter Guetens[1], Ana Moreno-Murillo[1], Yarno Valgaerts[1], T. Edwig Traoré[4], D. Florence Ouedraogo[4], Halidou Tinto[4], Ann Van de Velde[5], Alfred Cortés[6,7], Guy Caljon[3], Anna Rosanas-Urgell[1*]

[1] Department of Biomedical Sciences, Institute of Tropical Medicine, Antwerp, Belgium

[2] Department of Clinical Sciences, Institute of Tropical Medicine, Antwerp, Belgium.

[3] Laboratory of Microbiology, Parasitology and Hygiene (LMPH), Infla-Med Centre of Excellence, University of Antwerp, Belgium.

[4] Unité de Recherche Clinique de Nanoro, Institut de Recherche en Sciences de la Santé, Nanoro, Burkina Faso.

[5] Hematology and Hemostasis Unit, Universitair Ziekenhuis Antwerpen (UZA), Antwerp, Belgium.

[6] ISGlobal, Barcelona, Catalonia, Spain.

[7] ICREA, Barcelona, Catalonia, Spain.

* Corresponding author

E-mail: arosanas@itg.be (ARU)

ABSTRACT

Malaria transmission relies on the differentiation of asexual parasites into gametocytes, a process initiated by sexual conversion (SC). Mutations in the host hemoglobin beta (HBB) gene are known to influence parasite growth and disease outcome, yet their impact on SC remains unclear. We investigated the effect of HBB mutant genotypes on *Plasmodium falciparum* SC and humoral immunity in individuals from Nanoro, Burkina Faso. To measure SC rates in natural human malaria infections, we developed a new *ex vivo* SC assay (*ev*SCA). We found that in human natural *P. falciparum* infections, SC rates were higher in individuals with HbAS or HbAC than in individuals with wild-type HBB (HbAA). Consistently, using an *in vitro* SC assay (*iv*SCA) based on the NF54-*gexp02-Tom* reporter line we found that cultures grown in HbAS red blood cells (RBCs) had higher SC rates than those grown in HbAA RBCs. Furthermore, IgG and IgM responses against trophozoite- and stage I gametocyte-infected RBC antigens, quantified by flow cytometry, did not differ between plasma from individuals with different HBB genotypes. These results demonstrate that exposure to RBCs with HBB mutations enhances SC, highlighting a host-genetic factor that may influence malaria transmission potential.

AUTHOR SUMMARY

Transmission of *Plasmodium falciparum* –a malaria causing parasite− depends on the parasite's ability to produce gametocytes, the stage that infects mosquitoes. In many African regions where malaria is common, hemoglobin (Hb) variants such as hemoglobin S (the sickle-cell trait) and C are highly prevalent reflecting their role in protecting against severe disease. However, it remains unclear whether these variants also influence the parasite's early shift toward gametocyte development (*i.e.,* sexual conversion [SC]). In this study, we combined *ex*

49 *vivo* and *in vitro* SC assays to measure SC in red blood cells with different hemoglobin
50 genotypes. We found that SC was higher in parasites growing in red blood cells carrying
51 hemoglobin AC and AS genotypes compared to normal AA hemoglobin. These findings
52 provide experimental support for earlier epidemiological observations reporting that
53 individuals with these hemoglobin variants often carry more gametocytes and are more
54 infectious to mosquitoes. We also measured antibody levels in individuals with mutant RBCs
55 and found no differences in immunity that could explain the variation in SC. Our results show
56 that host genetic background can influence gametocyte development and may shape the
57 infectious reservoir in high-burden settings. This knowledge is important for designing
58 effective strategies for malaria elimination.

59 INTRODUCTION

60 *Plasmodium falciparum* (*P. falciparum*) causes over half a million deaths annually, mostly in
61 young children from low- and middle-income countries. Despite the substantial progress in
62 reducing the global malaria burden during the last decade, this decline has stalled, with some
63 countries reporting a resurgence in clinical cases [1]. Innovative approaches for malaria control
64 and elimination are thus urgently needed.

65 *Plasmodium* infections have exerted strong evolutionary pressure on the human genome, with
66 hemoglobin mutations providing a well-documented example [2-5]. Mutations in the human
67 HBB gene, such as hemoglobin S (HbS) and hemoglobin C (HbC), result from a substitution
68 of glutamic acid at position 6 with valine in HbS and lysine in HbC. Individuals can carry
69 homozygous (HbSS or HbCC), heterozygous (HbAS or HbAC) or compound heterozygous
70 (HbSC) mutations [6-8]. HBB mutations lead to significant changes in RBC morphology and
71 function, influencing malaria susceptibility and clinical outcomes [5, 9, 10]. HbS mutations
72 induce hemoglobin polymerization under low oxygen, causing RBCs to reshape into sickle

73 forms. HbSS causes ~60-80% RBC sickling [2] with severe complications including vaso-
74 occlusion, hemolysis, and chronic anemia [11, 12]. This results in early-life mortality, with
75 estimates ranging from 50-90% among children in low-and middle income countries [13]. On
76 the other hand, HbAS carriers are typically asymptomatic [2], with fewer sickled RBCs (~40%)
77 [12, 14]. HbC mutations cause hemoglobin crystallization without sickling but increase blood
78 viscosity and shorten RBC life span [15]. HbCC and HbAC are usually a mild and
79 asymptomatic disorder, with HbCC occasionally causing mild chronic hemolytic anemia in
80 some individuals [2, 7, 15]. HbSC carriers display moderate disease severity and a mixed
81 phenotype with ~50% sickled/crystallized and "pita-shaped" RBCs [2, 11, 16].

82 HbSS is relatively rare (~2%), likely due to its high mortality, whereas HbCC, although a mild
83 disorder, is also relatively uncommon (~2%). HbAS and HbAC can reach frequencies of 10-
84 30% in regions such as Mali and Burkina Faso, which has been linked to the protection they
85 confer against *P. falciparum* malaria [4, 5, 8, 17-20]. HbAC offers mild protection against
86 severe malaria, whereas HbAS and HbCC provide strong protection against both
87 uncomplicated and severe malaria [5, 15, 21-23]. How different HBB mutations protect against
88 malaria is not fully understood, but several mechanisms have been proposed [4, 24-31]. HbS
89 infected-RBCs (iRBCs), especially in HbSS, exhibit elevated heme and HO-1−mediated
90 oxidative stress. This causes polymerization, disrupts the actin cytoskeleton, alters iRBCs
91 morphology, and impairs the surface expression of *P. falciparum* erythrocyte membrane
92 protein 1 (PfEMP1) on iRBCs [32-34]. In HbAS iRBCs, this reduces cytoadherence and
93 sequestration, promoting splenic clearance and controlled parasite infection [25, 35].

94 Beyond protection from disease, HbS and HbC RBCs may influence the transmission potential
95 of *P. falciparum*. Population-based studies have reported conflicting evidence regarding
96 whether HbAS influences gametocyte carriage. Some studies reported no significant
97 association between HbAS and increased gametocyte carriage, while HbAC and HbCC were

98 associated with increased gametocyte carriage in the same [36] and other populations [37]. In
99 contrast, other studies found a link between HbAS and gametocyte carriage [38-40]. Some
100 studies have also reported higher infectivity to mosquitoes in individuals carrying HbAS [36,
101 37, 40], HbAC [36, 37] and HbCC [36] compared to wild-type HbAA iRBCs.

102 Gametocyte production is initiated by a process called sexual conversion (SC), in which a
103 variable but typically small proportion (~1%) of asexual *P. falciparum* parasites commit to
104 sexual development at each replication cycle, a proportion referred to as the SC rate (SCR),
105 and initiate gametocytogenesis [41-43]. Sexual commitment is marked by epigenetic activation
106 of the master regulator *pfap2g*, a transcription factor that irreversibly results in SC and
107 gametocyte development [44-47]. Sexual rings circulate in blood [48-51], while maturation of
108 gametocyte stages I to IV occurs mainly in the bone marrow over ~10 days [52]. Mature male
109 and female stage V gametocytes re-enter the peripheral blood, resulting in gametocyte carriage,
110 and are the only parasite stages capable of infecting *Anopheles* mosquitoes. Gametocyte
111 carriage determines human to mosquito transmission and correlates with infectivity to
112 mosquitoes [53-58].

113 The elevated gametocyte carriage reported in individuals with HbAC [36, 37] and, in some
114 studies, HbAS genotypes [38-40] could result from elevated SC but also from prolonged
115 infections, leading to accumulation of gametocytes in peripheral blood over numerous
116 replication cycles. Several host related factors have been shown to increase SC [59], including
117 lysophosphatidylcholine depletion [60-62], reticulocyte-rich environments [63, 64], and
118 antimalarial treatment [65-68]. However, other studies did not find enhanced SC after
119 antimalarial treatment [67]. To date, the link between SC and HBB genetics has been explored
120 to a limited extent, with one study reporting that increased intracellular heme in HbS iRBCs
121 promotes SC [32]. Another potential driver of elevated SC in HBB mutant RBCs is the host
122 immunity against *P. falciparum*. HbS and HbC mutations appear to modulate host immunity

123 against *P. falciparum* by increasing regulatory cytokines (*e.g.,* IL-10) [30], upregulating HO-1
124 [28], and dampening pro-inflammatory responses (*e.g.,* TNF-α, IFN-γ) [24], which both protect
125 against severe malaria and enhance parasite clearance. While there is evidence of a differential
126 humoral immune response between different HBB genotypes, differences were only detectable
127 in certain populations and for very specific antigens [69-73].

128 Discrepancies in gametocyte carriage studies highlight the need to investigate upstream
129 processes such as SC. Determining if HBB mutant RBCs enhance *P. falciparum* SC could
130 confirm that carriers of these mutant RBCs are key contributors to the infectious reservoir – as
131 proposed by mosquito feeding studies [36, 37, 40], informing strategies to reduce transmission.

132 In this study, we investigated the impact of host HBB mutant genotypes (HbAA, HbAC, HbAS,
133 HbSS, HbCC and HbSC) on SC in naturally infected malaria patients and *in vitro P. falciparum*
134 cultures and on IgG and IgM reactivity against trophozoite- and stage I gametocyte-infected
135 RBCs (iRBCs) by flow cytometry.

136 RESULTS

137 HbAC and HbAS genotype prevalences in Nanoro, Burkina Faso

138 Using Sanger Sequencing, the HBB gene was genotyped in participants of a longitudinal cohort
139 study (*i.e., InHost* study [74]) in Nanoro, Burkina Faso ($n = 864$) and the population frequencies
140 of HbAA, HbAC, HbCC, HbAS, HbSS, and HbSC genotypes were determined (Fig 1). HbAA
141 (wild-type) was the most frequent (71.5%), followed by HbAC (20%), HbAS (7.7%), HbSC
142 (0.8%), and HbCC (0.2%). No HbSS individuals were identified.
143

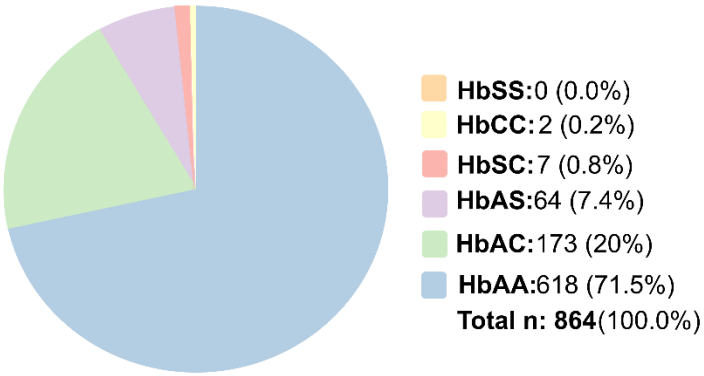

144

145 **Fig 1. Genotype frequencies of the HBB gene in the study population.** Pie chart depicting the total number of individuals (n) and frequencies (%) of the different HBB genotypes in the study population.

146 Novel *ex vivo* assay reveals elevated sexual conversion in 147 HbAS/HbAC

148 To investigate the effect of HBB genotypes on *P. falciparum* SC we measured SCRs *in vivo* in
149 *P. falciparum* isolates collected from naturally infected individuals with different HBB
150 genotypes (14 HbAA, 12 HbAC, and 6 HbAS) living in the malaria-endemic area of Nanoro,
151 Burkina Faso (Fig 2). For this, we developed a new *ex vivo* SC assay (*ev*SCA), optimized and
152 validated as described in *S1 Appendix*. In brief, to assess the proportion of circulating rings in
153 infected individuals that are sexual or asexual, parasites were cultured *ex vivo* in the presence
154 of the PKG inhibitor ML10 (to prevent reinvasion [75]) until the majority of parasites reached
155 the schizont stage. At this time, sexual rings have progressed to Pfs16-positive stage I
156 gametocytes. Next, parasites were concentrated using magnetic columns, and thin blood smears
157 were prepared from the enriched fractions. SCRs were quantified by immunofluorescent
158 staining (IFAs) detecting the proportion of parasites that stained positive for Pfs16 (stage I
159 gametocytes) [76-78] relative to the total number of parasites, stained for DNA/parasite nuclei
160 (the total parasite population consisting of stage I gametocytes plus schizont stages) [45, 79,
161 80]. The experimental set-up of the *ev*SCAs and representative IFA images are shown in Figs

162 2A and 2B, respectively. The median SCR was 2.65% (IQR 1.72) in *P. falciparum* isolates
163 from HbAA genotype, 5.05% (IQR 2.55) for HbAC and 18.40% (IQR 19.70) for HbAS
164 genotypes. SCR increased modestly in HbAC (beta-binomial generalized linear mixed model
165 [GLMM], odds ratio (OR)[95%CI] = 1.82 [1.17-2.82], *p (Bonferroni)* = 0.0032) and strongly
166 in HbAS (beta-binomial GLMM, OR [95%CI] = 8.16 [4.34-15.37], *p (Bonferroni)* < 0.0001)
167 genotypes compared to HbAA (Fig 2C, S1A Table). The fold-change between median SCR of
168 *P. falciparum* isolates in HbAC and HbAS relative to the median SCR of wild-type HbAA
169 RBCs was 2.04 (IQR 0.85) in HbAC and 7.07 (IQR 7.32) in HbAS, reflecting the increased
170 SCRs in HbAC and HbAS RBCs compared to HbAA.
171

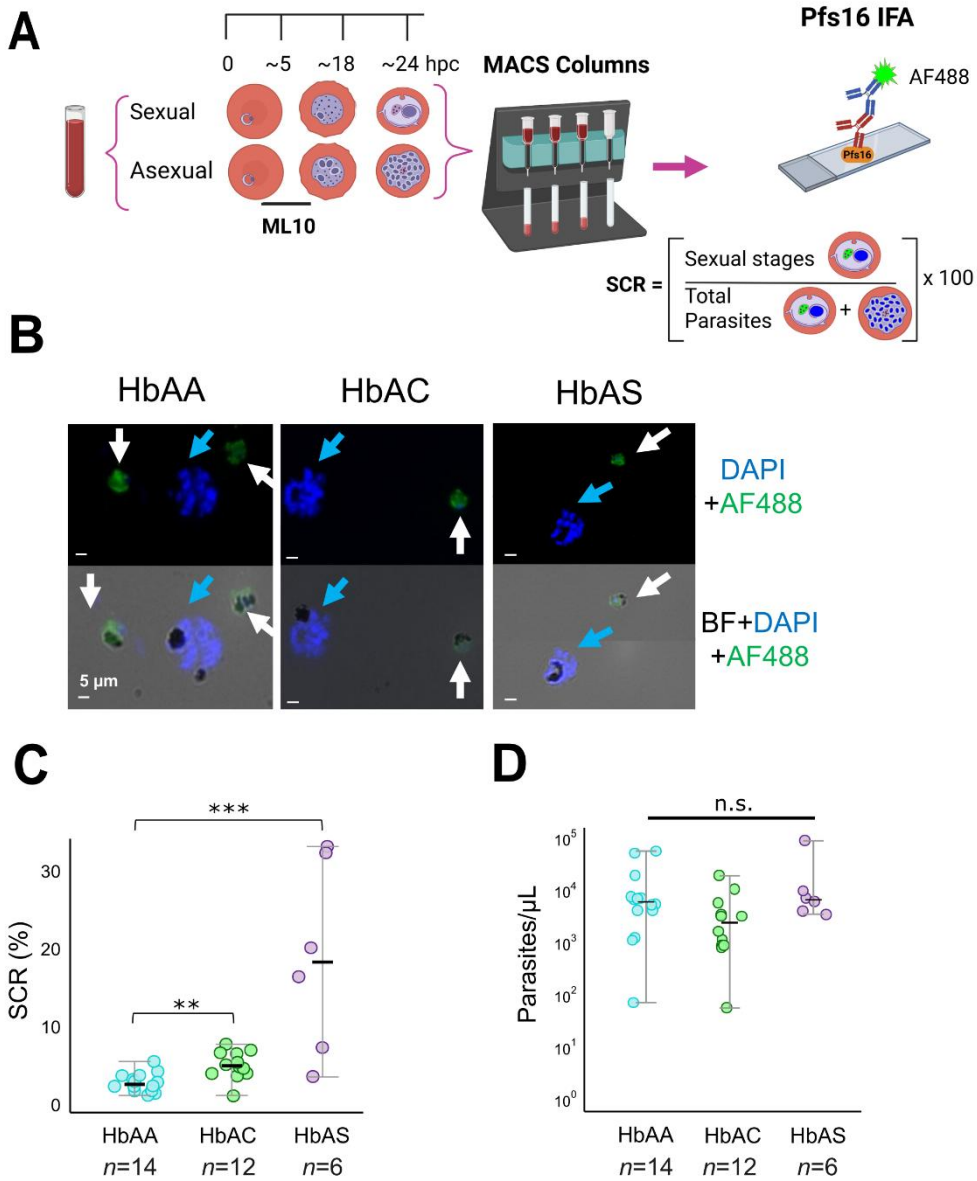

Fig 2. Effect of HbAA, HbAC and HbAS on SC determined with *ex vivo* SC assays. (A) Schematic representation of the *ex vivo* SC assays (*ev*SCAs). Parasite isolates from RBCs with different HBB genotypes cultured *ex vivo*, ML10 added at 11 hpi., MACS-enriched stage I gametocytes and schizonts detected by IFA Pfs16 (sexual stages) and DAPI (total parasites) staining. SCR (%): number of sexual stages/number of total parasites. **(B)** Representative IFA images of parasites in HbAA, HbAC and HbAS RBCs. Top row with DAPI (all parasites; blue arrows: schizonts) and AF488 (white arrows: stage I gametocytes) overlay and bottom row including brightfield (BF) channel to visualize the parasite's hemozoin. Objective: 40×; Scale bar: 5µm. **(C)** SCRs by HBB genotype determined using IFA. Individual dots, represent the mean SCR of three independent technical IFA replicates from one culture; the horizontal line and error bars indicate the median SCR and IQR of all cultures from the same HBB genotype. **(D)** Initial parasitemia at 0 hpc by HBB genotype **Statistical tests: C,** Beta-binomial GL(M)M with per-genotype dispersion parameter and Bonferroni correction for pairwise comparisons; **D,** Kruskal-Wallis test. Significant ($p < 0.05$*, $p < 0.01$**, $p < 0.001$***) and non-significant p-values (ns). **Abbreviations**: AF, Alexa Fluor; DAPI, 4',6-diamidino-2-phenylindole; GL(M)Ms, Generalized linear (mixed) models; Hb, hemoglobin; HBB, human hemoglobin beta; Hpc, hours post culture; hpi, hours post-invasion; IFA, immunofluorescence assays; ML10, cGMP-dependent protein kinase inhibitor; RBCs, red blood cells; SC, sexual conversion; SCR, sexual conversion rate.

174 Parasitemias did not significantly differ between mutant HBB RBCs (HbAC and HbAS) and
175 wild-type HbAA RBCs (Kruskal-Wallis test, overall $p = 0.72$, Fig 2D); and SCRs and initial
176 parasitemia did not correlate (Spearman correlation, $\rho = 0.05$, $p = 0.62$; (S1A Fig). These results
177 indicate that differences in initial parasitemias do not have an impact on the observed elevated
178 SCRs. A risk analysis of different variables in the study population (*i.e.,* gender, village,
179 ethnicity, age, parasitemias, etc.) across HBB genotype groups, showed that SCRs is the only
180 variable that significantly differs amongst the HBB genotypes HbAA, HbAC and HbAS
181 (Kruskal-Wallis test, overall $p < 0.001$; S2 Table).
182

183 *In vitro* sexual conversion in red blood cells of different HBB 184 genotypes

185 To confirm the findings from the *ev*SCAs, we adapted a previously described *in vitro* SC assay
186 (*iv*SCA) [65] to investigate SC in mutant RBCs (Fig 3A). The assay is based on the *P.*
187 *falciparum* transgenic reporter line NF54-*gexp02-Tom* [65, 81], which carries an integrated
188 tandem Tomato (tdTom) fluorescent marker under the control of the promoter of the early
189 gametocyte marker gene *gexp02*. Percoll-purified schizonts were grown in cryopreserved
190 RBCs with different HBB genotypes from 28 wild-type and mutant donors, including 15
191 donors from the malaria-endemic area of Nanoro, Burkina Faso (5 HbAA, 5 HbAC, 4 HbAS,
192 and 1 HbSC) and 13 patients with hemoglobinopathies (12 HbSS and 1 HbSC) from a non-
193 endemic area (Antwerp University Hospital). In addition, non-cryopreserved (fresh) RBCs
194 from 6 control HbAA donors (HbAA CTRL) from a non-endemic area were included (Fig 3A).
195 After 5 h, sorbitol lysis was performed to achieve tight synchronization (5 h age window) and
196 cultures were maintained either with (+Choline) or without (-Choline) a choline supplement,
197 to measure basal or induced SCRs, respectively [60, 79, 81]. At the next cycle (Generation 1),

198 SCRs were estimated as the proportion of total parasites (identified by Hoechst33342 staining)
199 that developed as sexual forms (TdTom positive), determined by flow cytometry [81]. A
200 previous report described that the vast majority of sexual parasites expressed the TdTom
201 reporter from 10-15 hpi of Generation 1 onwards [81], and other studies using this assay
202 typically measured SCRs at 20-25 hpi [65]. However, to account for the possible
203 developmental delay observed in cultures grown in RBCs with mutant HBB (see next section),
204 we also measured SCRs at 35-40 hpi. The *iv*SCA assay (Fig 3A, S2 Fig) was validated for use
205 with cryopreserved mutant RBCs as described in the *S1 Appendix*. As detailed in the Methods,
206 analyses were intentionally restricted to parsimonious models due to sample size constraints,
207 and results should be interpreted accordingly.

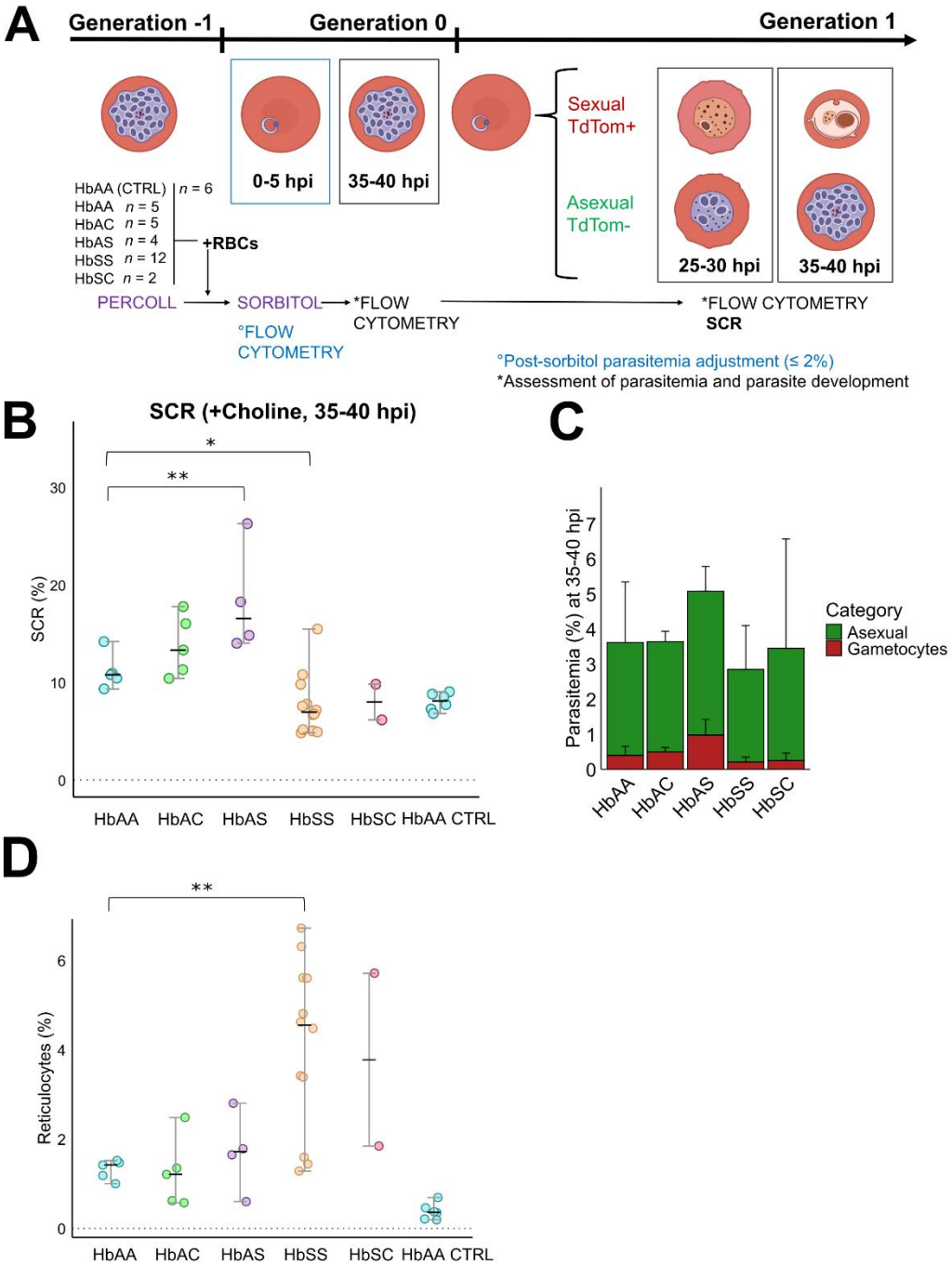

Fig 3. Effect of HbAA, HbAC, HbAS, HbSS and HbSC on SC by *in vitro* SC assays. (A) Experimental design of *in vitro* SC assays (*iv*SCAs) using the NF54-*gexp02-Tom P. falciparum* line. Tightly synchronized schizonts (Generation -1) were allowed to reinvade RBCs of different HBB genotypes, and ring stages (0-5 hpi) were cultured under non-inducing (+Choline) and inducing (-Choline) conditions. Parasite development was assessed by flow cytometry at 35-40 hpi (Generation 0) and 25-30 hpi/35-40 hpi (Generation 1). SCRs were measured by flow cytometry at 25-30 hpi and 35-40 hpi (Generation 1). **(B)** SCRs by HBB genotype at 35-40 hpi (Generation 1) in +Choline cultures. **(C)** Proportion of asexual and gametocyte stages and total parasitemia by HBB genotype at 35-40 hpi (Generation 1) in +Choline cultures. **(D)** Reticulocytes percentage by HBB genotype. **Statistical tests:** B and D, Beta-binomial GLMs with Bonferroni correction for pairwise comparisons. Significant *p*-values are shown as: $p < 0.05$*, $p < 0.01$**, $p < 0.001$***; non-significant *p*-values as: ns. **Abbreviations:** CTRL, control sample; GLMs, Generalized linear models; Hb, hemoglobin; HBB, human hemoglobin beta; Hpi, hours post-invasion; SC, sexual conversion; SCR, sexual conversion rates.

221 In non-induced cultures (+Choline), SCRs measured at 35-40 hpi were significantly higher in
222 HbAS RBCs than in wild-type HbAA RBCs (median 16.50% vs. 10.80%, OR[95% CI] = 1.73
223 [1.12−2.66], *p* [*Bonferroni*] = 0.0056 using beta-binomial GLM) (Fig 3B, S1B and S3 Tables).
224 The same trend was observed for HbAC RBCs, but in this case the difference was not
225 significant (median 13.30%, *p[Bonferroni]* = 0.77 using beta-binomial GLM; S1B Table). In
226 contrast, SCRs were significantly lower in HbSS RBCs (median 6.96%, OR[95% CI] = 0.64
227 [0.43−0.95], *p* [*Bonferroni*] = 0.021 compared to HbAA RBCs, using beta-binomial GLM) and
228 non-significantly lower in HbSC RBCs (median 7.99%, *p[Bonferroni]* = 0.62, using beta-
229 binomial GLM) (Fig 3B, S1B and S3 Tables). The fold-changes between median SCR in
230 HbAC, HbAS, HbSS and HbSC relative to the median SCR of wild-type HbAA RBCs were
231 1.24 (IQR 0.44) in HbAC, 1.53 (IQR 0.53) in HbAS, 0.65 (IQR 0.29) in HbSS and 0.74 (IQR
232 0.17) in HbSC RBCs, reflecting the increased SCRs in HbAC and HbAS RBCs compared to
233 HbAA. The same trends were observed when SCRs were measured at 25-30 hpi, but in this
234 case none of the differences were statistically significant (S3A Fig, S1B and S3 Tables).
235 However, SCRs estimated at 25-30 hpi were generally lower than at 35-40 hpi (S3 Table),
236 supporting the idea that some sexual parasites had not started expressing TdTom yet at 25-30
237 hpi. Therefore, we considered that, in our experiments with cryopreserved RBCs, measuring
238 SCRs at 35-40 hpi was more appropriate. This is also supported by the results presented in the
239 next section, showing a developmental delay associated with some HBB genotypes.

240 In cultures in which SC had been stimulated by choline depletion (-Choline), SCRs were
241 significantly lower in cultures with HbSS or HbSC RBCs than in cultures in HbAA RBCs at
242 both 25-30 hpi and 35-40 hpi (beta-binomial GLM; S1B Table). At 25-30 hpi, median SCRs
243 were 24.00% in HbAA cultures, compared with 16.00% in HbSS (OR[95% CI] = 0.52
244 [0.35−0.79], *p[Bonferroni]* = 0.0003) and 10.20% in HbSC (OR[95% CI] = 0.36 [0.17−0.77],
245 *p[Bonferroni]* = 0.0032). At 35-40 hpi, SCRs increased in HbAA cultures (median 35.50%)

246 but remained lower in HbSS (median 18.40%, OR[95% CI] = 0.41 [0.27−0.61], *p[Bonferroni]*
247 < 0.0001) and HbSC cultures (median 11.90%, OR[95% CI] = 0.30 [0.14−0.64], *p[Bonferroni]*
248 = 0.0003) (S3B and S3C Figs, S3 Table). While the reduced SCRs observed in HbSS and HbSC
249 RBCs under both basal and inducing conditions may reflect impaired SC associated with these
250 HBB genotypes, it is also possible that these results are explained by parasite developmental
251 arrest in these RBCs. On the other hand, in choline-depleted cultures, SCRs were similar in
252 HbAS or HbAC RBCs compared with HbAA RBCs (Figs S3B and S3C, S1B and S3 Tables),
253 indicating that the high SCR observed after choline depletion does not further increase in
254 mutant HBB RBCs.

255 The final total parasitemia (Generation 1) followed a similar trend as final gametocytemia
256 between all genotypes, highest in cultures with HbAS RBCs and lowest in HbSS and HbSC
257 RBCs (Fig 3C, S3D Fig). This indicates successful reinvasion of all RBC types, and confirms
258 that the higher SCRs in HbAS reflect enhanced gametocyte production rather than reduced
259 asexual parasite numbers. Furthermore, differences in SCRs could not be explained by
260 variation in initial parasitemia at 0-5 hpi (Generation 0, all cultures were adjusted to a
261 parasitemia below 2.0%), as no significant differences were found between HBB genotypes
262 (beta-binomial GLM, p *[Bonferroni]* = 1; S1B Table). Additionally, no correlation was
263 observed between SCR and initial parasitemia (Spearman $\rho = 0.10$, $p = 0.63$; S1B Fig). We
264 assessed other possible confounders for the differences in SCR among HBB genotypes. A risk
265 analysis of different variables in the study population (HBB genotype, ABO blood group,
266 gender, village and ethnicity) confirmed that HBB genotypes are a risk factor for enhanced
267 SCRs, in addition to gender (females) (Fisher's exact test, overall $p < 0.01$ and $p < 0.05$,
268 respectively; Table 1). Gender was not included in further analyses due to its imbalanced spread
269 across HBB genotypes (S4 Table). Since reticulocytes have been proposed to enhance SCRs
270 [63], and individuals with mutant HBB genotypes often exhibit anemia-associated

271 reticulocytosis, we assessed reticulocyte percentages across all HBB genotypes. We observed
272 significantly higher reticulocyte percentages in HbSS compared to HbAA RBCs (beta-
273 binomial GLM, OR [95%CI] = 2.56 [1.20−5.44], *p [Bonferroni]* = 0.008, S1B Table and Fig
274 3D), which was confirmed in a risk analysis of reticulocytes, amongst other factors, across
275 HBB genotype groups (Kruskal-Wallis test, overall $p < 0.001$; S4 Table). SCRs across HBB
276 genotypes were negatively correlated with reticulocyte percentage (Spearman $\rho = -0.50$, $p <$
277 0.01; Table 1). Since SCR could not be readily measured in HbSS and HbSC genotypes due to
278 parasite developmental delay/arrest in these RBCs (see next section), we performed correlation
279 analysis without the HbSS and HbSC genotypes, only between HbAA, HbAC and HbAS. No
280 correlation was observed between reticulocyte percentage and SCR (Spearman $\rho = 0.10$, $p =$
281 0.73; S3E Fig), suggesting that higher SCRs are likely due to intrinsic properties of mutant
282 RBCs rather than to higher reticulocyte abundance. Lastly, to control for hemolysis during the
283 assays, we assessed RBC counts (RBCs/µl) across HBB genotypes at various timepoints, as
284 shown in S5 Table. No significant differences were observed at any of the time points,
285 indicating that mutant HBB RBCs did not undergo hemolysis during the course of the
286 experiment.

287

Table 1. **Risk analysis of factors associated with elevated SCRs in the *in vitro* SC assays.**

Median (IQR)	SCR at 35-40 hpi (Generation 1)	*p*-value$
HBB genotype		<0.01
HbAA	10.8 (0.49)	
HbAC	13.30 (4.71)	
HbAS	16.50 (5.64)	
HbSS	6.96 (3.17)	
HbSC	7.99 (1.83)	
ABO blood group		0.15
O+	7.57 (7.86)	
A+	8.80 (2.52)	
B+	17.80 (3.48)	
A-	9.34 (2.87)	
B-	10.90 (3.77)	
Gender		<0.05
Female	11.30 (3.75)	
Male	7.57 (4.09)	
Village		0.30
Nanoro	11.30 (3.75)	
Nazoanga	15.40 (0.60)	
Soum	0 (0.00)	
Séguédin	0 (0.00)	
Ethnicity		0.40
Gourounsi	17.80 (0.00)	
Mossi	12.30 (4.14)	
	Median (IQR)	***p*-value (rho)°**
Reticulocytes (%)	1.50 (5.63)	< 0.01 (-0.50)
Age	27.00 (30.00)	0.37 (-0.18)
***n* (%)**	28 (100.00)	-

Significant p-values ($p < 0.05$*, $p < 0.01$**, $p < 0.001$***). $Categorical variables test: Fisher's exact test, Continuous variables test: Kruskal Wallis test, °Continuous variables: Spearman correlation test.
SCRs measured at 35-40 hpi (Generation 1). Data from *P. falciparum* non-infected samples collected in Nanoro, Burkina Faso and the Antwerp University Hospital (UZA, Belgium) (total $n = 34$). Statistical tests performed are shown at the bottom of the figure with correspondent significant *p*-values as: $p < 0.05$*, $p < 0.01$**, $p < 0.001$***). **Abbreviations:** Hb, hemoglobin; HBB, human hemoglobin beta; hpi, hours post-invasion; IQR, Interquartile range; *iv*SCAs, *in vitro* sexual conversion assays; SCRs, sexual conversion rates.

288

289 # Red blood cells with mutant HBB genotypes delay parasite
290 # development

291 *P. falciparum* growing in HbAS RBCs exhibits developmental delay/arrest before DNA
292 replication when growing under low oxygen conditions (≤ 5% O_2, as present in the bone
293 marrow and spleen, and in standard *P. falciparum* cultures as used for the *iv*SCA) [25].

294 Developmental delay/arrest in a particular HBB genotype would affect the time at which SC
295 can be measured *in vitro.* To characterize in more detail the possible alterations in parasite
296 development when grown in RBCs with different genotypes, we first quantified the percentage
297 of rings, trophozoites and early/late schizonts in a set of cultures with the different HBB
298 genotypes using light microscopy (LM) at three timepoints (35-40 hpi at Generation 0; 25-30
299 hpi at Generation 1; and 35-40 hpi at Generation 1) (Fig 4A). Parallel analysis of the proportion
300 of late stages (schizonts) in the same samples by flow cytometry revealed consistent patterns
301 between the two approaches (Fig 4B). We therefore used flow cytometry (gating strategy in
302 Fig 4C) to analyze parasite development in all RBC samples. Samples with very low late-stage
303 proportions (at 35-40 hpi) likely reflect slow development (remaining in early stages), rather
304 than rapid development to ring stages in the next generation.
305 Parasite developmental delay was estimated by comparing parasite stage distributions and
306 mean parasite age to wild-type HbAA cultures, using the expected timing of the
307 intraerythrocytic cycle (~44 h) to approximate the corresponding delay in hours. Delay versus
308 (partial) arrest was defined based on consistent deviations from HbAA cultures across multiple
309 LM- and flow cytometry-derived parameters, including late-stage proportions at successive
310 time points and their change between generations (Fig 3A), as well as parasite multiplication
311 rates, allowing classification of individual cultures as expected, delayed, or (partially)
312 arrested/extremely delayed development (S6 Table). Detailed analysis is further described in
313 *S1 Appendix.* We found that parasites in HbAA RBCs progressed normally from Generation 0
314 to 1 with no apparent delay; however, there was unexpected high variability between individual
315 donors (Fig 4B). In HbAC RBCs, parasite development was slightly delayed (~3 hours delay
316 vs. HbAA at Generation 0, 35-40 hpi) but without arrest. In contrast, HbAS RBCs showed a
317 more pronounced delay (~10 hours), with partial developmental arrest observed in one sample
318 (Figs 4A and 4B, S6 Table). HbSS and HbSC RBCs presented a similar delay to HbAS (~9

319 and ~16 hours delay, respectively) with a persistent population of schizonts, trophozoites, and
320 late rings across all timepoints (Fig 4A), consistent with the high frequency of partially
321 arrested/delayed cultures (67% in HbSS and 50% in HbSC) (S6 Table). The (partial)
322 arrest/extreme delay in these cultures potentially makes them unsuitable for SCR measurement
323 and may explain the apparent reduction in SCRs associated with growth in RBCs with these
324 genotypes. These results confirm the convenience of measuring SCRs at 35-40 hpi in this
325 experimental set-up.

326

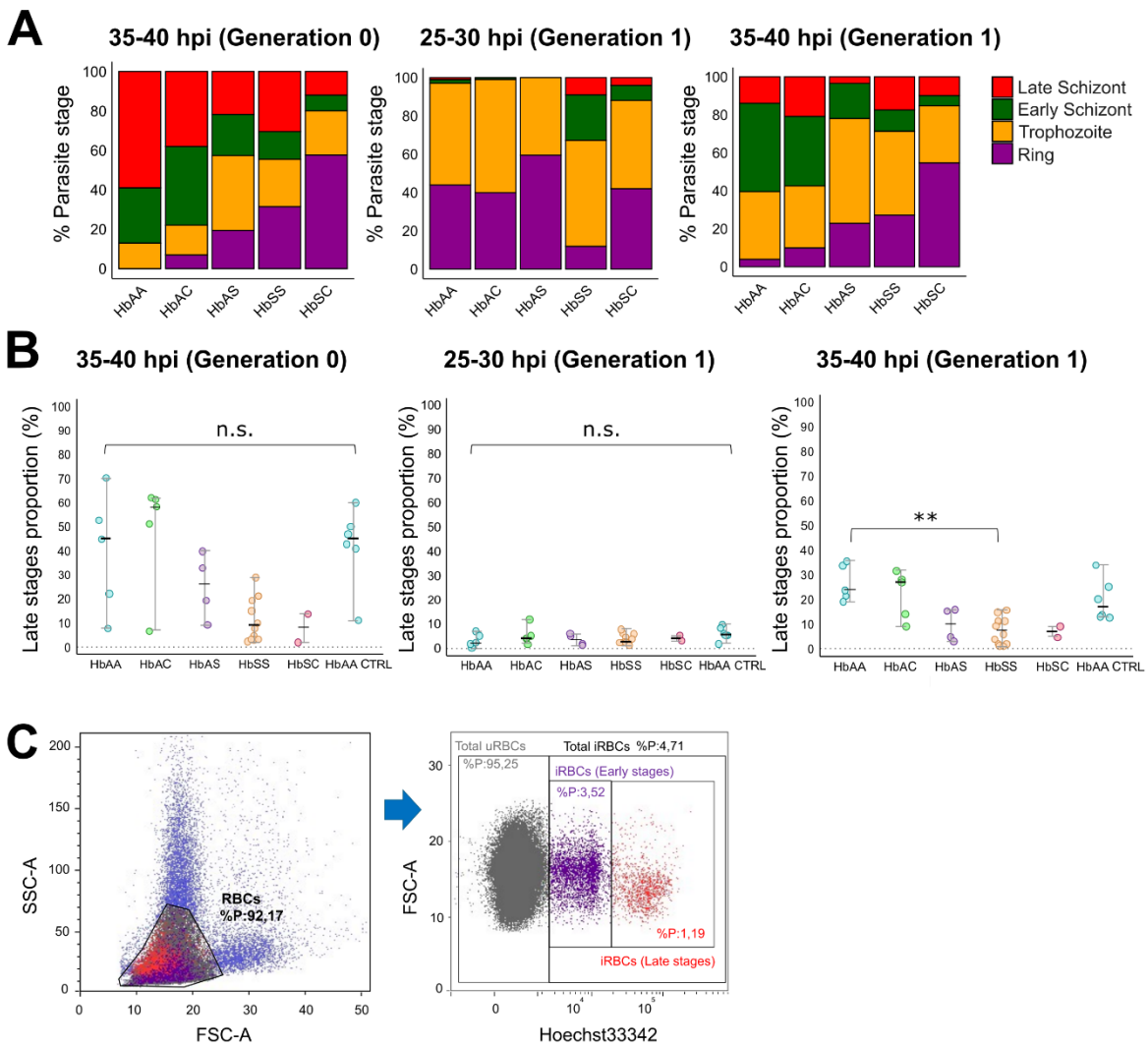

327

Fig 4. *P. falciparum* parasite development in RBCs with different HBB genotypes. (A-B) Timepoints shown are: 35-40 hpi (Generation 0; left graph), 25-30 hpi (Generation 1; middle graph) and 35-40 hpi (Generation 1; right graph). **(A)** Microscopy-based quantification of parasite stages expressed as percentages of a total of 100 counted parasites per sample. Y-axis: percentage of parasite stages (%); X-axis: HBB genotype groups (HbAA $n = 1$, HbAC $n = 1$ and HbAS $n = 2$, and HbSS $n = 2$ and HbSC $n = 2$ donors from a malaria-endemic area in Nanoro, Burkina Faso. **(B)** Proportion of late stages (*i.e.,* schizont stages) on the total infected RBCs (iRBCs) by flow cytometry (Y-axis) by HBB genotype groups (X-axis) (HbAA $n = 5$, HbAC $n = 5$ and HbAS $n = 4$, and HbSC $n = 1$ donors from a malaria-endemic area in Nanoro, Burkina Faso; HbSS $n = 12$, HbSC $n = 1$ and $n = 6$ control HbAA donors [HbAA CTRL] from a non-endemic area). **(C)** Representative flow cytometry plots showing the gating strategy for the detection of late parasite stages. Left: total RBCs gated. Right: within the total RBCs gate in left plot, uninfected RBCs (uRBCs) and iRBCs are identified, with iRBCs further gated into early and late parasite stages by Hoechst 33342. **Statistical tests**:(B, right graph) beta-binomial GLM with Bonferroni correction for pairwise comparisons; (B, left and middle graph) Kruskal-Wallis test. Significant ($p < 0.05$*, $p < 0.01$**, $p < 0.001$***) and non-significant p-values (ns). **Abbreviations:** CTRL, control sample; FSC-A, Forward Scatter-Area; GLMs, Generalized linear models; Hb, hemoglobin; HBB, human hemoglobin beta; Hpi, hours post-invasion; RBCs, red blood cells; SSC-A, Side Scatter-Area.

328

329 **IgG and IgM reactivity in plasma of individuals with different**
330 **HBB genotypes**

331 We analyzed IgG and IgM reactivity against *P. falciparum* in individuals with different HBB
332 genotypes using flow cytometry and selected plasma samples from humans living in the
333 malaria-endemic area of Nanoro, Burkina Faso, collected as part of the *InHost* longitudinal
334 cohort study [74] (see *Materials and methods*). IgG and IgM antibodies were measured against
335 antigens on the surface of intact RBCs infected with the *P. falciparum* transgenic reporter line
336 NF54-*gexp02-Tom* [65, 81] at the early trophozoite / gametocyte stage (20-25 hpi; Generation
337 1; Fig 3A) using a flow cytometry protocol adapted from Dantzler KW., et al., (2019) [82].
338 Plasma samples from individuals living in malaria-endemic area were defined as "endemic
339 plasma", whereas samples from individuals living in non-endemic area were defined as "non-
340 endemic plasma". Detailed information on assay optimization and validation is provided in the
341 *S1 Appendix.* Flow cytometry gates were set to quantify total iRBCs (trophozoites and stage I
342 gametocytes), asexual iRBCs (trophozoites), and sexual iRBCs (stage I gametocytes) based on
343 Hoechst33342 and tdTomato (tdTom) fluorescence. IgG- and IgM-positive cells were
344 identified using AF488 and PerCP-Cy5.5, respectively, resulting in six populations: total
345 iRBCs (Hoechst+/tdTom+ or -), asexual iRBCs (Hoechst+/tdTom-), and sexual iRBCs
346 (Hoechst+/tdTom+), each subdivided by IgG- or IgM-positivity (S4B Fig). To ensure robust
347 ΔMean Fluorescence Intensity (ΔMFI) measurements, a minimum number of 200 IgG- or IgM-
348 positive iRBCs (events) per gated population was required. This cut-off refers to the number
349 of antibody-positive cells contributing to the ΔMFI calculation (Figs S5A and S5C).

350 In each assay, positive controls including three acute *P. falciparum*-infected non-endemic
351 plasma samples from a traveler at days 0 (D0), 21 (D21) and 23 (D23), and a negative control
352 ("naïve non-endemic plasma") were analyzed. Endemic plasma samples were considered

353 positive for IgG or IgM when both the event count and IgG- and IgM-positive total-iRBC
354 proportions exceeded those observed in the "naïve non-endemic plasma". The "naïve non-
355 endemic plasma" sample consistently did not reach the 200 event counts threshold, confirming
356 its suitability as a negative control. The negative control values served as a baseline for the
357 IgG- and IgM-positive total iRBC proportions (% cells) and were lower than those of the
358 endemic plasma samples of all HBB genotypes (Fig 5). Importantly, the events count of IgM-
359 positive total and asexual iRBCs in the positive controls at D21 and D23 exceeded both the
360 event counts observed in the "naïve non-endemic plasma" and the threshold of 200 events,
361 confirming that our flow cytometry assay can detect IgM-positive total and asexual iRBCs
362 (S5C Fig). The time course of the "acute *P. falciparum*-infected non-endemic plasma at D0,
363 D21 and D23" generally followed the expected IgG (D0 < D21 < D23) and IgM (D0 < D21 >
364 D23) dynamics in IgG- and IgM-positive total iRBCs after a *P. falciparum* infection [83, 84].

365 MFI could only be evaluated for IgG-positive total and asexual iRBCs in the statistical analyses
366 (Figs S5B and S5D), because all endemic plasma samples (n = 61) exhibited event counts
367 below 200 for the IgM and IgG-positive sexual iRBCs, thirteen samples (21%) had no detected
368 (*i.e.,* zero) events for IgM-positive sexual iRBCs and the median event count of IgM-positive
369 total and asexual iRBCs was below the 200 event threshold for all HBB genotype groups. The
370 percentage of IgG- or IgM-positive iRBCs reflects the proportion of iRBCs recognized by
371 antibodies, whereas the MFI reflects the relative level of antibody binding per positive cell.
372 When IgM-positive sexual iRBCs were rare or absent, the proportion of positive cells could
373 still be quantified, but MFI could not be reliably estimated due to insufficient antibody-positive
374 events.

375

376

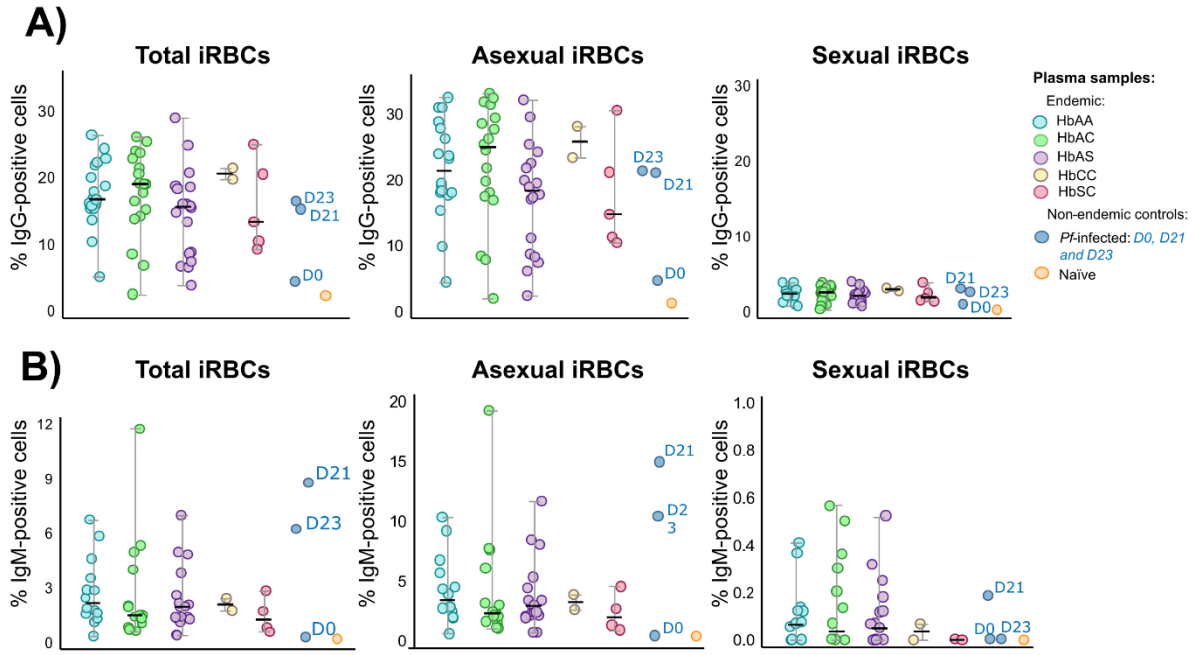

377

Fig 5. IgG- and IgM-mediated responses to *P. falciparum* trophozoites and stage I gametocytes across HBB genotypes. Data from *P. falciparum* infected (n = 44) and non-infected (n = 17) plasma samples collected at the Clinical Research Unit (CRUN) in Nanoro, Burkina Faso (total n = 61). **(A)** Percentage of IgG-positive iRBCs: total (left), asexual (middle) and sexual (right) iRBCs. **(B)** Percentage IgM-positive iRBCs: total (left), asexual (middle) and sexual (right) iRBCs. Positive controls ("*Pf*-infected non-endemic" *i.e.,* three acute *Pf*-infected non-endemic plasma samples from a traveler at D0, D21, and D23) and a negative control *i.e.,* "Naïve non-endemic": non-endemic plasma from a volunteer with HbAA genotype) are shown as individual dots per sample. The Y-axis range differs between graphs for visualization. No significant differences were found (beta-binomial GLM with Bonferroni adjustment for pairwise comparisons, $p > 0.05$). **Abbreviations:** asexual iRBCs, trophozoites; D, day(s); GLM, Generalized linear models; Hb, hemoglobin; HBB, human hemoglobin beta; IgG and IgM, Immunoglobulin G and M; iRBCs, infected-red blood cells; *Pf, P. falciparum*; sexual iRBCs, stage I gametocytes; total iRBCs, trophozoites and stage I gametocytes.
378

379 In endemic plasma samples, we detect low or absent IgG- and IgM-positive sexual iRBC
380 proportions, and low or absent IgM-positive total and asexual iRBC proportions, as compared
381 to high IgG-positive total and asexual iRBC proportions (Figs 5 and S5). We found no
382 significant differences in the IgG- and IgM-positive total iRBC proportions (% of cells/ΔMFI
383 data are only considered robust for IgG-positive total and asexual iRBCs, reaching the
384 minimum threshold of 200 events; Fig 5) (beta-binomial GLM, $p > 0.05$; S1C Table). When
385 analyzing the response against sexual or asexual iRBCs separately, there was no significant
386 difference across endemic plasma from individuals carrying different HBB genotypes in IgG-

387 or IgM-positive asexual or sexual iRBC proportions (Fig 5, S7 Table) (beta-binomial GLM, p
388 > 0.05; S1C Table).

389 The evaluation of variables in the study population (n = 61) such as: *P. falciparum* infection
390 status at the time of sample collection, parasitemia (parasites per µl), presence of gametocytes
391 in blood, age, gender and village; across HBB genotype groups (HbAA [n = 18], HbAC [n =
392 18], HbAS [n = 18], HbCC [n = 2], and HbSC [n = 5]) revealed no significant differences
393 between categories (Fisher's exact test and Kruskal-Wallis test; p > 0.05; S8 Table). In our
394 study population, there is a homogeneous distribution of individuals across the categorical
395 variables, with no observed sampling bias that could affect further analysis (S8 Table).
396 Further analysis of the IgG- and IgM-positive total iRBC proportions by "*P. falciparum*
397 infection status", showed higher antibody recognition in infected individuals (n = 44) compared
398 to non-infected individuals (n = 17) (S6 Fig). IgG-positive total iRBC proportions were
399 markedly higher in infected individuals (median[IQR]: 17.90[6.30]) than in non-infected
400 individuals (9.10[9.66]) (beta-binomial GLM, OR[95%CI] = 1.81[1.35−2.43], p = 0.001; S1C
401 Table). In contrast, IgM-positive total iRBC proportions showed only a modest increase in
402 infected individuals (2.03[3.34]) compared to non-infected individuals (1.56[1.27]) (beta-
403 binomial GLM, OR[95%CI] = 1.51[1.01−2.23], p = 0.043; S1C Table). These results confirm
404 the expected IgM dynamics, where IgM-positive iRBC proportions are highest during acute or
405 recent infections (*P. falciparum*-infected individuals) compared to past infections (non-
406 infected individuals) [83, 84].
407 Stratification analysis of the IgG- and IgM-positive total iRBC proportions by age-group (*i.e.,*
408 younger age: "1 to 4 years" compared to older age: "5 to 19 years") in *P. falciparum*-infected
409 compared to non-infected individuals, showed that both *P. falciparum*-infected and non-
410 infected individuals with younger age had lower IgG-positive total iRBC proportions (*Pf*-
411 infected n = 22 and median[IQR]: 17.90[7.23]; non-infected n = 15 and median[IQR]:

412 9.30[10.80]) than those with an older age (*P. falciparum*-infected n = 22 and median
413 [IQR]:18.60[5.64]; non-infected n = 2 and median[IQR]: 12.60[3.69]) (Welch's ANOVA, p =
414 0.082 [IgG]; Kruskal-Wallis test, p = 0.38 [IgM]). *P. falciparum*-infected individuals with
415 younger age had slightly higher IgM-positive total iRBC proportions (n = 22, median [IQR]:
416 2.19[2.33]) than those with an older age (n = 22, median [IQR]: 1.87[3.04]) (Kruskal-Wallis
417 test, p = 0.94). In contrast, the IgM-positive total iRBC proportions in non-infected individuals
418 with younger age were slightly lower (n = 15, median[IQR]: 1.56[1.12]) than those with an
419 older age (n = 2, median [IQR]: 2.18[0.00]) (Kruskal-Wallis test, p = 0.16).
420 Overall, these findings demonstrate that the flow cytometry assay accurately detects IgM-
421 positive asexual iRBC proportions, as validated by positive controls, whereas such responses
422 are rare or absent in individuals from endemic areas (Fig 5). The increase of IgG with age and
423 decrease of IgM with age explains the low IgM-positive total iRBC proportions in the endemic
424 plasma: exposure leads to a build-up of immunity that replaces low-affinity IgM by an affinity-
425 matured IgG response [84-88].

426 DISCUSSION

427 This study demonstrates that *P. falciparum* SC is significantly influenced by host hemoglobin
428 genotype. SC was higher in HbAS RBCs than in wild-type HbAA RBCs both in natural
429 infections *in vivo* and *in vitro* (using the *P. falciparum* transgenic reporter line NF54-*gexp02-*
430 *Tom*), whereas a slight increase was observed for HbAC RBCs *in vivo* that could not be
431 confirmed *in vitro*. This genotype-dependent modulation of SC was accompanied by a
432 developmental delay in parasites within HbS- and HbC-infected RBCs (iRBCs). However, we
433 found no differences in IgG or IgM responses against trophozoite- and early gametocyte-iRBC
434 surface antigens across HBB genotypes. Together, these findings indicate that host RBC
435 intrinsic properties, rather than humoral immunity, underly altered parasite reproductive
436 strategies in HBB mutant backgrounds.

437 Amoah et al., (2020) [89] analyzed the effect of HBB genotype on SC of field isolates from
438 Ghanaian children aged 6-15 years with uncomplicated malaria, and reported a non-significant
439 trend of decreasing SCRs from HbAA to HbAC and HbAS. The discrepancy with our results
440 is most likely methodological, because quantifying SC in natural infections is challenging as
441 parasites in freshly collected blood include morphologically indistinguishable sexual and
442 asexual rings. The authors used prolonged culture (≥4 days) to distinguish sexual stages from
443 asexual forms, similarly to Usui et al., (2019) [49]. The limitation of this approach is that SCRs
444 are measured as the ratio of stage II gametocytes on day 4 (D4) by the total parasitemia on day
445 0 (D0). This can underestimate SCR because parasites contributing to the denominator (D0)
446 are counted before culture adaptation affects viability, whereas the numerator (D4) includes
447 only gametocytes that survive and mature after several days in *ex vivo* conditions, during which
448 parasite loss can occur.

449 We addressed these limitations by adapting an *ev*SCA to quantify SC [45] for experiments with
450 mutant RBCs. We measured whether infection of individuals with RBCs with different HBB
451 genotypes leads to alterations of sexual conversion rates. We quantified the proportion of
452 parasites in patient samples that differentiated as asexual or sexual forms after *ex vivo*
453 maturation. Quantification is done by immunofluorescence, with stage I gametocytes detected
454 by Pfs16 IFA and overall parasites by DAPI [80]. Key aspects for the success of our new
455 *ev*SCA were the inclusion of the PKG inhibitor ML10 that prevented reinvasion, allowing
456 numerator and denominator measurements for the SCR at the same time point, while
457 enrichment using LD columns improved sensitivity. This approach reliably quantified SC in
458 natural human infections with densities as low as 0.05% (~2,500 parasites/µl) and detected a
459 minimum of 38 stage I gametocytes per sample, with no gametocyte-negative cultures.

460 We confirmed the *in vivo* findings in the *ev*SCAs using an *in vitro* SC assay (*iv*SCA) with a
461 gametocyte reporter line [81], which allows early detection of sexual rings. In this assay,

462 parasites growing in HbAS RBCs showed higher SCRs than those in HbAA RBCs, whereas
463 parasites in HbSS and HbSC RBCs were associated with lower SCRs *in vitro*. For HbAC
464 RBCs, a slight increase observed although not statistically significant. The fold-change SCR
465 observed for HbAS relative to HbAA RBCs in the *iv*SCA was consistent with that reported by
466 Flage, B., et al., (2023) [32] (1.5 vs. 1.5 in HbAS), although the results are not directly
467 comparable due to clear methodological differences. In our assay, SCR was defined as the
468 proportion of *gexp02*-expressing parasites among total parasites in the next cycle (generation
469 1), whereas in Flage, B., et al., (2023) [32], sexual parasites were quantified at generation 1
470 and total parasitemia at generation 0, precluding direct comparison. For HbSS and HbSC
471 RBCs, strong conclusions regarding SCR cannot be drawn, as parasite development appeared
472 to be impaired after reinvasion and no corresponding data from natural infections were
473 available. This contrasts with findings in Flage, B., et al., (2023) [32], who reported markedly
474 higher SCRs in HbSS RBCs (35% vs. 6.96% in our study) and no apparent developmental
475 delay at day 2 of culture, although this was not quantitatively assessed. As noted above,
476 differences in the timing and approach used to quantify SCR make direct comparison between
477 studies difficult.

478 Parasite developmental progression differed across HBB genotypes and likely influenced SCR
479 estimation. We observed a partial developmental delay in parasites infecting HbAS and HbAC
480 RBCs, and a more pronounced arrest or extreme delay in HbSS and HbSC RBCs under low-
481 oxygen conditions (5% O_2), as assessed by both light microscopy and flow cytometry,
482 consistent with Archer, N.M., et al., (2018) [25]. Later time-point measurements at 35-40 hpi
483 resulted in higher SCRs in endemic HbAA, HbAC, and HbAS RBCs compared with 25-30 hpi,
484 suggesting delayed sexual marker expression and underestimation of SCR at earlier time points
485 due to developmental delay. In contrast, parasites grown in control non-endemic HbAA RBCs
486 showed stable SCRs across both time points. The differences observed between endemic and

487 non-endemic HbAA RBCs may reflect unmeasured host genetic factors, such as blood group
488 variants or other RBC polymorphisms.

489 Under choline-depleted conditions, SCRs in HbSS and HbSC increased modestly (from <10%
490 to 10-20%) but remained below levels in HbAA, HbAC, and HbAS RBCs (>30-40%). This
491 likely reflects severe developmental delay causing under-detection of sexually committed rings
492 at the measured time points rather than inhibited sexual commitment *per se*. Overall, our data
493 indicate that accurately assessing SC in HbSS and HbSC RBCs is challenging with this
494 experimental approach due to impaired parasite development. We further evaluated host-
495 related factors previously associated with SC, including reticulocyte abundance, parasitemia,
496 and ABO blood group [63-65, 90-94], but none of these potential confounders influenced SCRs
497 in either the *ev*SCA or *iv*SCA. Together, these results indicate that the observed increase in SC
498 is specifically associated with HBB genotype rather than these other host-related variables.
499 Interpretation of risk/GL(M)M analyses was limited by the small sample size and unbalanced
500 group structure in terms of potential confounding factors, which constrained model complexity
501 and precluded fully adjusted multivariable analyses. Although residual confounding or
502 interactions cannot be excluded, the direction and magnitude of the observed HBB genotype
503 effect were largely consistent across models, supporting its biological relevance.

504 The increase in SC in RBCs with HBB mutant genotypes *in vitro*, in the absence of plasma and
505 white blood cells, points to RBC-intrinsic effects rather than host immune responses or soluble
506 plasma factors as the most plausible cause for the altered SCR observed in HBB mutant RBCs.
507 HbS and HbC RBCs exhibit elevated levels of free heme [95], linked to increased oxidative
508 stress that leads to polymerization of HbS under low oxygen conditions [96], and delays
509 parasite development [25]. In Flage, B., et al., (2023) [32], authors showed that heme directly
510 induces SC. The oxidative stress inhibits actin polymerization in infected HbS and HbC RBCs
511 [34], which alters protein trafficking and PfEMP1 display [28, 31]. This reduces cytoadherence

512 [35], and membrane flexibility [97]. Oxidative stress also modifies RBC micro RNAs that can
513 hybridize with parasite mRNAs [27], directly affecting parasite development and metabolism,
514 and increasing gametogenesis [32]. Taken together, these findings suggest that the effect of
515 HbAC and HbAS RBCs on SC *in vitro* is likely driven by oxidative stress caused by free heme
516 within these RBCs, mediated by their specific miRNA profiles. The stronger effect *in vivo*,
517 particularly in HbAS (7.07-fold vs ~2.05- fold *in vitro*), probably reflects additional *in vivo*
518 factors such as parasite genetic diversity [49, 80], host factors not captured *in vitro* [80, 98],
519 although we cannot exclude that part of the difference may be attributable to variations in
520 experimental setup.

521 To further investigate potential *in vivo* influences, we assessed the humoral immune response
522 in the different HBB genotypes. Altered antigen presentation, cytoadherence, and increased
523 splenic clearance [35] could plausibly lead to an modified immune response in HbAC and
524 HbAS. However, epidemiological studies examining immunity in individuals with HbAS and
525 HbAC genotypes have yielded conflicting results. Older children with HbAS have been shown
526 to be more protected against the establishment of parasitemia, suggesting an acquired
527 mechanism of protection [29]. In contrast, another study found no differences in antibody
528 responses between individuals with HbAA, HbAS, and HbAC genotypes against their panel of
529 491 immunoreactive *P. falciparum* antigens [99]. More recent studies have shown that
530 serological responses tend to be differential in individuals with HbAC and HbAS when
531 focusing on specific surface antigens and populations [70-73].
532 Given that differences in serological responses appear specific to certain surface antigens, we
533 chose to measure IgG and IgM reactivity against intact iRBCs. This approach enables the
534 assessment of immune responses to native surface antigens, minimizing potential artifacts
535 arising from non-native protein folding, glycosylation, or conformation. We focused on
536 trophozoite-iRBCs (25-30 hpi), as surface antigen presentation (*i.e.,* PfEMP1 expression)

537 begins around 16 hpi and plateaus at approximately 24 hpi [100]. Moreover, commitment to
538 SC occurs between 17-37 hpi [45, 65], suggesting that any antibody-mediated induction of
539 sexual commitment would need to occur at this stage.
540 We compared IgG and IgM responses to trophozoite- and gametocyte-iRBCs using plasma
541 samples from Burkinabé individuals carrying HbAA, HbAC, HbAS, HbCC, and HbSC
542 genotypes, assessed by flow cytometry. Our analyses revealed no significant differences in IgG
543 or IgM reactivity against trophozoite- and stage I gametocyte-iRBCs across genotypes. IgM
544 responses, as well as responses against gametocyte-iRBCs, were generally low or absent.
545 Therefore, we could not confirm genotype-dependent differences in humoral responses to these
546 parasite stages and consider it unlikely that antibodies directly drive the differential SC
547 observed in these individuals. However, our analysis was limited to the antigens expressed by
548 the parasite reporter line used in the assay. Responses against the immunodominant variant
549 surface antigen PfEMP1 are notoriously difficult to decipher in *in vitro* systems as it is encoded
550 by approximately 60 different *var* genes which are expressed mutual exclusively [101] and
551 expression is significantly reduced *in vitro* compared to *in vivo* [102]. Moreover, we cannot
552 exclude the possibility that genotype-specific antibody responses to later parasite stages,
553 particularly during gametocytogenesis, as suggested by recent studies on gametocyte
554 antigenicity [82, 103], could influence transmission potential, either by promoting clearance of
555 developing gametocytes in the human host or by inducing gametocyte sterility within the
556 mosquito vector [104].

557 Overall, this study demonstrates elevated SC of *P. falciparum* parasites in HbAS and HbAC
558 RBCs both *in vitro* and in *ev*SCAs − measuring SC in natural human infections *in vivo*. For
559 HbAC RBCs, however, the results were less clear: differences in SC were smaller in both
560 natural infections and *in vitro*, and the *in vitro* differences were not statistically significant,
561 indicating the need of additional studies. These findings further support the view that *P.*

562 *falciparum* can adjust its reproductive investment in response to stress-related cues. In mutant
563 HBB RBCs, elevated levels of free heme can induce developmental delay and thereby
564 compromise survival within the human host; increased investment in SC may thus represent a
565 parasite survival strategy [25, 32, 105].

566 Previous studies have shown that microenvironmental factors such as LysoPC depletion,
567 nutrient limitation and exposure to antimalarial drugs can modulate malaria transmission by
568 changing the parasite's SCR. How factors such as free heme translate into a signal received by
569 epigenetic regulators controlling the sexual commitment genes *ap2-g* or *gdv1* remains an open
570 question [32, 45]. At the population level, HBB mutant genotypes have been linked to increased
571 gametocyte carriage and higher mosquito infectivity. In Burkina Faso, a two- to four-fold
572 higher infection rates in HbAS, HbAC, and HbCC carriers was reported [36]. Similar trends
573 were observed in Mali and Cameroon, where HbAC and HbAS individuals carried more
574 gametocytes and were more infectious to mosquitoes than HbAA [37, 40]. These population-
575 level associations are consistent with our findings, and suggest that increased SC in mutant
576 HBB RBCs may contribute to their enhanced transmission potential.

577 MATERIALS AND METHODS

578 Details about reagents and tools are available in S9 Table.

579 Study design

580 Sample collection for the present study was embedded in a longitudinal cohort study assessing
581 the effect of host factors on transmission potential (*InHost* study, ethical advice reference
582 1261/18 and 19/06/064), conducted in the Nanoro health district, a rural malaria-hyperendemic
583 region, in the Central-West of Burkina Faso (Fig 6)[74]. Briefly, 871 study participants of all
584 ages from four villages (Nanoro, Nazoanga, Séguédin and Soum) of the district were followed-

up for two years (March 2019 - February 2021) through six cross-sectional surveys conducted during both high and low transmission season to assess asexual and sexual parasite carriage and risk factors. Active case detection was complemented by passive case detection at peripheral health centers.

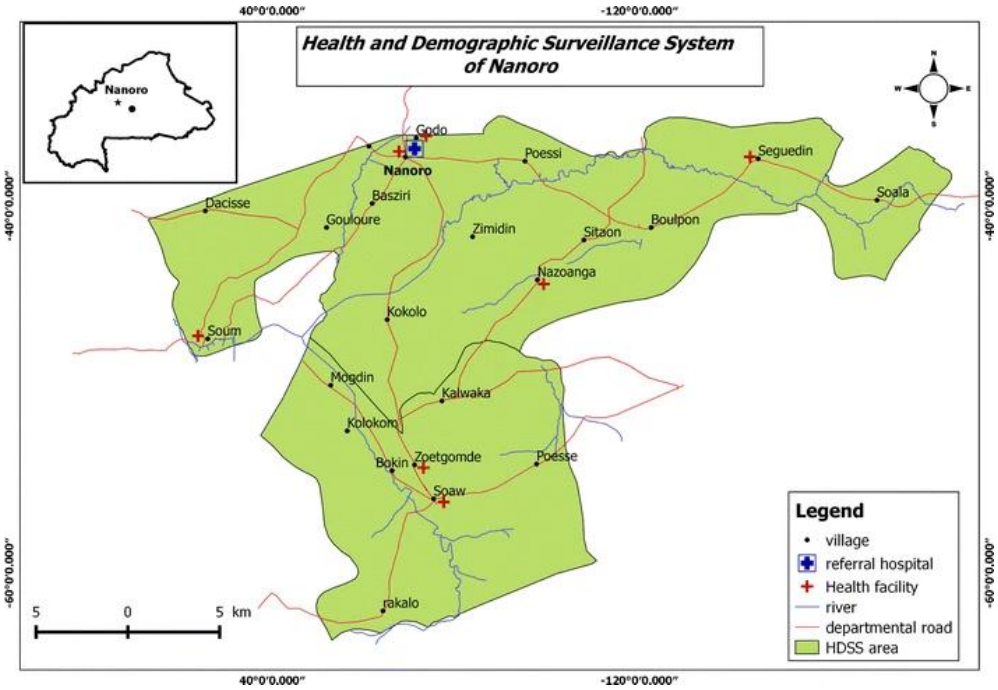

Fig 6. Map of the study area. The inset map highlights the location of the Nanoro health district of Boulkiemdé Province in Central Burkina Faso, with the black dot indicating the position of the capital, Ouagadougou.

For this study, from all participants of the *InHost* study (n = 871), 864 individuals were genotyped for their human HBB genotype (see section on "Hemoglobin beta sequencing"). Participants were then selected for this sub-cohort based on their genotype. A venous blood sample was collected from all selected participants, and screened for *P. falciparum* infection. Samples from *P. falciparum*-infected individuals were used to perform *ex vivo* SC assays (*ev*SCAs) and samples from non-infected individuals were preserved to perform *in vitro* SC assays (*iv*SCAs). We included all individuals carrying the HBB genotypes HbAC (n = 72), HbAS (n = 50), HbCC (n = 2), HbSC (n = 7), and a random subset of individuals with the HbAA genotype (n = 94) (S7 Fig). In total, 225 individuals were listed (age groups "5 - 19 years" [n = 166] and "more than 20 years" [n = 59]). Listed individuals were visited by a nurse

601 at home and were invited to the Clinical Research Unit of Nanoro (CRUN, Burkina Faso) for
602 screening and enrolment into the study. Population screening for *P. falciparum* infections and
603 enrolment took place over a two-month period (August-September 2022).
604 At CRUN, the eligibility was assessed based on inclusion and exclusion criteria for the *ev*SCAs
605 (*P. falciparum*-infected individuals) and *iv*SCAs (non-infected individuals). Inclusion criteria
606 consisted of: being enrolled in the main *InHost* study, a confirmed *P. falciparum* malaria
607 infection (for the *ev*SCAs) or a confirmed negative *P. falciparum* malaria infection (for the
608 *iv*SCAs), willing to participate in this study and undergo additional sampling, and signed
609 informed consent. Exclusion criteria consisted of: mixed infection with other *Plasmodium*
610 species (only for *P. falciparum*-infected individuals in the *ev*SCAs), antimalarial treatment
611 within the last two weeks, signs of severe malaria (*e.g.* prostration), severe chronic illness
612 besides hemoglobinopathies (*e.g.,* cancer, heart disease, kidney or liver disorders, HIV/AIDS,
613 etc.), and planning to leave the study region during the study period. Of the 225 listed
614 individuals, 162 were screened at CRUN, of whom 161 participants were selected as eligible
615 and were included within this sub-cohort (S7 Fig). A 15 ml venous blood sample was collected
616 from each participant. After sample collection, blood samples were screened for *P. falciparum*
617 infections (see section on "*P. falciparum* diagnosis"). Samples with confirmed *P. falciparum*
618 infection and parasitemia by light microscopy (LM) ≥ 0.05% (*i.e.* ≥ 2500 parasites/µl) were
619 processed for *ev*SCAs at CRUN (Table 2). Blood samples negative for *P. falciparum* infection
620 were processed and preserved for *iv*SCAs conducted at the Institute of Tropical Medicine
621 (ITM), Antwerp (Table 2, see section on "*iv*SCAs"). *P. falciparum*-infected individuals, as
622 detected by LM and confirmed with *P. falciparum var* gene acidic terminal sequence (*var*ATS)
623 quantitative PCR (qPCR), were treated with Artemether-Lumefantrine (AL) following national
624 guidelines and were asked to return three days later to confirm infection clearance.

625 Sample size was calculated based on a power analysis assuming an expected effect size of 50%,
626 a 5% significance level, and 90% power. This sample size was considered sufficient to detect
627 differences in SC by HBB genotype, based on effect sizes reported in previous studies [63]. To
628 account for potential variability in HBB genotype groups, a minimum of 8 participants per
629 HBB genotype group was required. To ensure sufficient sampling and successful assays per
630 HBB genotype group, the sample size was upscaled to a maximum of 15 participants per HBB
631 genotype group.

632 To increase the number of HbSC and HbSS blood samples for *iv*SCA, additional blood samples
633 were collected from patients with hemoglobinopathies (HbSS and HbSC) visited at the
634 Antwerp University Hospital (UZA), Belgium. A total of 13 adults (aged 19-37 years),
635 routinely followed at UZA's Hematology Unit, were invited to donate a blood sample with
636 exclusion criteria of fever. The inclusion period was between October 2023 and April 2024.

637 **Table 2. Number of samples (*n*) per *Plasmodium falciparum* infection status and donor HBB genotype at**
638 **collection.** Information given for the *ex vivo* SC assays (*ev*SCAs), *in vitro* SC assays (*iv*SCAs) and
639 Immunoglobulin (Ig) detection assays.
640

	HbAA	HbAC	HbAS	HbSC	HbCC	HbSS	Total
EvSCAs							
Pf+ (CRUN, total *n*)	14	12	6	-	-	-	32
IvSCAs							
Pf- (total *n*)	5	5	4	2	-	12	28
CRUN (*n*)	5	5	4	1	-	-	
UZA (*n*)	-	-	-	1	-	12	
Ig detection							
Pf+ (CRUN)	13	13	13	3	1	-	43
Pf- (CRUN)	5	5	5	2	1	-	18
Total n (*Pf+* and *Pf-)*	18	18	18	5	2	-	61

641 Note: *P. falciparum-infected (Pf+)* samples used in the *ev*SCAs must have a parasitemia ≥ 0.05% (*i.e.,* ≥ 2500
642 parasites/µl), as the established limit of accurate assessment of SC with these assays. **Abbreviations:** CRUN,
643 Clinical Research Unit in Nanoro; Hb, hemoglobin; ITM, Institute of Tropical Medicine in Antwerp; *Pf, P.*
644 *falciparum*; UZA, Antwerp University Hospital.

645 *Plasmodium falciparum* diagnosis

646 *P. falciparum* malaria diagnosis was done by RDT using the Bioline™ malaria antigen P.f®
647 test (05FK50, Abbott) (recommended by the National malaria Control Programme (NMCP) in
648 Burkina Faso), following the manufacturer instructions. In addition, malaria parasites were

649 detected and quantified by LM following standard protocols at CRUN [106]. In brief, venous
650 blood smears were stained with Giemsa and examined until 200 white blood cells were
651 counted. Parasitemia was calculated based on the number of asexual parasites per white blood
652 cells, expressed as asexual parasites per microliter of blood, assuming a white blood cell count
653 of 8,000 per microliter. The presence of gametocytes and other *Plasmodium* species (*P. ovale*
654 *and P. malariae*) was assessed in all positive blood smears [107]. Blood samples that tested
655 positive for *P. falciparum* by both RDT and LM were classified as *P. falciparum*-infected.
656 Samples that were negative by LM (regardless of the RDT result), were identified as non-
657 infected (Table 2, S7 Fig). Negative infection with *P. falciparum* was confirmed by *var*ATS
658 qPCR, using five µl of DNA (extracted with QIAamp DNA Mini Kit, Qiagen Germany), as
659 previously described [108, 109] (S7 Fig). The limit of detection of the *var*ATS qPCR was 0.1
660 parasite/µl (in our hands), with samples showing Ct > 39.7 considered negative. DNA from the
661 *P. falciparum* 3D7 strain served as a positive control, while negative controls included DNA
662 from non-infected human blood and a no-template control (NTC).

663 Sample collection and processing

664 At CRUN, a 15 ml venous blood sample was collected in an Acid Citrate Dextrose (ACD) tube
665 and the residual blood in the needle was used for *P. falciparum* diagnosis by RDT and LM (see
666 section on "*P. falciparum* diagnosis"). The sample was then immediately transported to the
667 laboratory for processing. Samples were centrifuged (1,648 g for 5 minutes) and washed two
668 times with RPMI to isolate the RBC pellet. RBC pellets from *P. falciparum*-infected blood
669 samples were immediately put in culture for the *ev*SCAs (see section on "*Ex vivo* SC assays
670 (*ev*SCAs)". RBC pellets from non-infected samples were cryopreserved (1:3 dilution in
671 cryopreservation solution containing 3% sorbitol and 0.65% NaCl) and stored directly at -80°C
672 until shipment to ITM, where preserved in liquid nitrogen until use in *iv*SCAs. Two hundred

673 microliters of whole blood were used for DNA extraction and confirmation of *P. falciparum*
674 infection by *var*ATS qPCR (see section on "*P. falciparum* diagnosis). At UZA, 15-20 ml of
675 non-infected venous blood samples were collected in EDTA tubes and immediately transported
676 at 4°C to ITM for processing, done as described at CRUN. The resulting RBC pellets were
677 cryopreserved (1:3 dilution in cryopreservation solution containing 3% sorbitol and 0.65%
678 NaCl) by direct snap-freezing in liquid nitrogen for subsequent *iv*SCAs. Additionally, ABO
679 and Rhesus D blood groups were determined with agglutination tests (BIO-RAD, REF:
680 801320, 801345, 802032).

681 Hemoglobin beta sequencing (HBBseq)

682 In samples collected at CRUN, PCR amplification of the HBB gene (NCBI_Gene:3043) was
683 performed to identify single nucleotide polymorphisms (SNPs) using PCR conditions adapted
684 from Wittwer CT,. et al., (2020)[110] and MMV & WHO [111]. Primer pairs were designed
685 to amplify a 599 bp product (S9 Table). PCR reactions were performed in a total volume of 25
686 µl, containing 2.5 µl of DNA template, 10× Buffer B, 5 mM of each dNTP, 0.3 µM of each
687 primer, 25 mM of $MgCl_2$, and FIREPol® DNA Polymerase (Solis Biodyne, Ref: 01-01-00500).
688 Thermal cycling conditions were as follows: an initial denaturation at 94°C for 6 minutes,
689 followed by 40 cycles of 60.6°C for 30 seconds, and 72°C for 1 minute, with a final extension
690 at 72°C for 10 seconds. After Sanger sequencing, chromatograms were analyzed using BioEdit
691 7.2. (Informer Technologies) to identify the wild-type and the mutant HBB codons (Table 3).
692 In samples collected at UZA, the HBB genotype sequences were determined by capillary
693 hemoglobin electrophoresis at UZA as described elsewhere [112].
694

695 **Table 3. HBB codons and genotypes identified by Sanger sequencing analysis of the HBB gene (HBB-seq).**

HBB allele	Mutation	HBB codon
HbA (wild-type)	-	GAG
HbS (mutant)	***c.20A>T = E (Glu)> V (Val)***	GTG
HbC (mutant)	***c.19G>A = E (Glu) > K (Lys)***	AAG
HbSC (double mutant)	***HbS mutation (Glu→Val) + HbC mutation (Glu→Lys)***	AAG + GTG [113]

696 **Abbreviations:** Hb, hemoglobin ; HBB, human hemoglobin beta.

697 *Ex vivo* sexual conversion assays

698 *Ex vivo* sexual conversion in *Plasmodium falciparum* field isolates

699 *P. falciparum*-infected fresh venous blood samples (15 ml) were collected from individuals
700 carrying different HBB genotypes (Table 2; HbAA n = 14, HbAC n = 12, HbAS n = 6; total n
701 = 32) and were cultured *ex vivo* to measure SCRs in natural human infections. Assay
702 optimization and validation described in *S1 Appendix*. Cultures at 3% Hct and 20 ml volume
703 were prepared by mixing 600 µl of *P. falciparum*-iRBC pellet with 20 ml of RPMI 1640
704 medium containing 0.5% Albumax II (Gibco, 11021-029) and 2 mM choline chloride (Sigma-
705 Aldrich, C7527) [65, 81]. Parasites at the ring stage were incubated using candle jar method
706 under static conditions until ~24 hours post-culture (hpc). At this time, sexually committed
707 rings present in the venous blood sample are expected to have developed into stage I
708 gametocytes expressing Pfs16, while asexual parasites will have progressed to the schizont
709 stage (Fig 2A). During culture, at ~5 hpc, ML10 (80 nM), a cGMP-dependent protein kinase
710 inhibitor, was added to prevent schizont rupture and reinvasion [45, 75]. Giemsa-stained
711 smears were examined by LM to confirm that most parasites had reached either stage I
712 gametocytes or schizonts stages. At ~24 hpc, parasites were harvested and purified using

713 MACS LD columns (Miltenyi Biotec). In brief, cultured parasites are centrifuged (1,648 g, 5
714 min) and pelleted iRBCs were diluted 1:4 with culture medium, loaded onto an LD-MACS
715 column, and washed four times with 1 ml medium to separate non-iRBCs and ring-stage-iRBCs
716 (first elution). The column was then removed from the magnet, and stage I gametocytes and
717 schizonts were recovered by gravity elution, followed by gentle plunger flushing twice with 3
718 ml medium (second elution). Recovered parasites were pelleted (1,648 g, 5 min), resuspended
719 1:2 with non-iRBCs, and diluted 1:2 in PBS. From the second elution, four thin blood smears
720 (3 µl each) were prepared and left to air-dry; three were used for on-site IFAs, and one was
721 Giemsa-stained for LM to verify MACS enrichment.

722 **Immunofluorescence assays**

723 Immunofluorescence assays (IFAs) were performed at CRUN (Burkina Faso) as previously
724 described [45, 65, 81], with modifications. Slides were stained in batches of four to eight
725 cultures with three slides per culture, to optimize processing and staining consistency. Primary
726 antibody mouse anti-Pfs16 (1:400, kindly provided by R. Sauerwein and T. Bousema, Radboud
727 University) [76] and secondary antibody goat anti-mouse IgG (H+L) Alexa Fluor 488 (1:1000;
728 Abcam, ab150113) were used, with incubations and washes under static conditions. Slides were
729 mounted with Aqueous Fluoroshield (Abcam, ab104139) containing DAPI (0.0002%) and
730 stored at 4°C until shipment to ITM (Belgium). At ITM, slides were visualized within six
731 months of preparation on an ECHO Revolve epifluorescence microscope (ECHO, San Diego,
732 CA) to determine SCRs (Fig 2B and 2C). Analysis was blinded to HBB genotype. Stage I
733 gametocytes were identified as Pfs16-positive cells (green) and counted among a minimum of
734 1,000 DAPI-positive cells (blue) per slide (stage I gametocytes and schizonts). Slides with
735 fewer than 1,000 DAPI-positive cells were excluded from further analysis during the first
736 reading. For each culture (n = 35), three of the four prepared slides were stained by IFA and

737 examined by a primary reader. Slides from three cultures were excluded due to insufficient
738 DAPI-positive cells. From the remaining cultures (n = 32) a random subset of ~10% (4/32),
739 with three IFA slides per culture, was examined by a second reader to assess inter-reader
740 reliability via intraclass correlation coefficient (ICC) analysis, based on a two-way random
741 effects model, absolute agreement, single measures [ICC(2,1) [114]]. For each IFA slide, SCRs
742 were calculated as the proportion of Pfs16-positive parasites among total DAPI-positive cells.
743 Across the three replicate IFA slides per culture, the mean SCR (±SD) was computed and used
744 to calculate and report the median SCR (IQR) by HBB genotype (Fig 2C), statistical differences
745 were assess as described for proportions in section "Data analysis". Fold-change in SCR for
746 HbAC and HbAS was calculated relative to HbAA by dividing each mutant genotype's median
747 SCR by that of the wild-type. Statistical analysis was performed to assess differences in SCRs
748 and in initial parasitemia across HBB genotypes (continuous not normally distributed
749 variables) (Figs 2C-D), as well as the potential confounding effect of initial parasitemia on
750 SCRs using non-parametric correlation (S1A Fig), as described in section "Data analysis".
751 Stable Pfs16 fluorescence was confirmed by the counting of ≥1 stage I gametocyte per 10
752 fields. For each culture, the three replicate IFA slides were analyzed to quantify SCRs. The
753 mean, minimum and maximum SCR were calculated across replicates. To assess inter-slide
754 reproducibility (technical repeatability) of SCR measurements, an ICC (2,1) analysis (two-way
755 random effects, single measures, consistency) was performed using SCR values from the three
756 replicate slides per culture (n = 32). Counts of stage I gametocytes and total parasites were
757 recorded for each IFA slide and summarized as median (Q1-Q3). From 5 out of 32 cultures
758 (15.6%) specificity controls were performed by staining one slide per culture without primary
759 antibody (negative controls). Stage V gametocytes (also express Pfs16), identified by their
760 shape, were excluded from the counting as they are a product of SC occurring >10 days prior
761 to the sexual commitment cycle under investigation. Giemsa-stained slides from each *ev*SCA

762 were examined by LM to estimate parasite purification by MACS and confirm approximate
763 parasite age/stage to assure parasites were sufficiently mature to express Pfs16 (starts
764 expression at ~20 hpi [45]).

765 *In vitro* sexual conversion assays

766 *In vitro* SC assays (*iv*SCAs) were performed as follows (Fig 3A). NF54-*gexp02-Tom* parasites
767 [65, 81] were routinely maintained with parasitemias of less than 2 % in O+ RBCs (3% Hct)
768 in RPMI 1640-based medium supplemented with 0.5% Albumax II (Gibco, ref: 11021-029)
769 and 2 mM choline chloride (+Choline; Sigma-Aldrich, C7527), analogous to LysoPC
770 supplementation [60, 79, 81]. Cultures were incubated at 37°C with shaking conditions (70
771 rpm) in a gas mixture (5% O_2, 5.5% CO_2, balance N_2). To minimize bias due to prior culture
772 duration, all cultures were initiated from parasites of the same cryopreserved batch of an
773 expanded culture.
774 To obtain cultures of a well-defined age window, we used Percoll/sorbitol synchronization (Fig
775 3A). Percoll-purified schizonts (Generation -1) were used to establish fresh cultures with
776 thawed cryopreserved RBCs (day 3 post thawing) with different HBB genotypes (exposure,
777 Generation 0), now cultured in static conditions. Thawing of RBCs was performed using a
778 three-step protocol, sequentially adding three volumes of 3.5% NaCl solution (10× the RBC
779 volume each time), followed by RPMI washes and centrifugation (1,648 g, 5 min) as per
780 standard procedure [115]. Approximately 5 hours later, when parasites have reinvaded the new
781 RBCs, cultures were subjected to 5% D-sorbitol lysis [45, 81] to obtain cultures of a defined
782 0-5 hpi age window. Post-sorbitol initial parasitemia was then measured by flow cytometry,
783 and parasites were cultured in two parallel subcultures (~200 µl final volume) per sample. One
784 sub-culture was maintained in +Choline medium (non-inducing SC conditions), and the other
785 in choline-free medium (-Choline; inducing conditions). Cultures were maintained under these

786 respective conditions for two generations (48 hpi, until 35-40 hpi in Generation 1, Fig 3A, hpi
787 calculations are based on a 44 hours replication cycle empirically established for this parasite
788 line in our lab). In each experiment we tested RBCs with at least two different HBB genotypes.
789 Samples with different HBB genotypes were used in the experiments if the recovered RBC
790 pellet volume after thawing was ≥ 30 µl after dilution with RPMI to 50% Hct. From a total of
791 20 cryopreserved non-iRBC samples from CRUN that were confirmed to be negative for *P.*
792 *falciparum* by *var*ATS qPCR, 15 samples had a RBC pellet volume ≥ 30 µl after thawing and
793 dilution in RPMI to 50% Hct (S7 Fig). The mean recovered RBC pellet volumes after thawing
794 were: HbAA, 178 µl (range: 50−596 µl); HbAC, 111 µl (range: 30−320 µl); HbAS, 246 µl
795 (range: 64−630 µl); HbSC, 558 µl (range: 35−1080 µl); and HbSS, 600 µl (range: 300−1120
796 µl). These samples were included within the *iv*SCAs, in addition to non-infected, cryopreserved
797 RBC samples from the UZA HbSS and HbSC (S7 Fig). Total numbers of samples tested per
798 HBB genotype and experiment are shown in S10 Table. Flow cytometry - analysis was used to
799 measure parasitemia, assess parasite stage development (*i.e.,* proportion of parasites reaching
800 the intraerythrocytic schizont stage or late-stage proportions), and quantify SC at defined time
801 points during the assay (Fig 3A). Parasitemia was determined at 0-5 hpi (rings), together with
802 (1) the proportion of schizont stages at 35-40 hpi in Generation 0 and 1, and (2) SCRs at 25-30
803 hpi (large rings/trophozoites) and 35-40 hpi (schizonts) in Generation 1 (Fig 3A). The standard
804 timepoint to measure SC with this parasite line is 25-30 hpi to ensure detection of all sexually
805 committed parasites, as TdTom-expression under the *gexp02* promoter starts around 10-15 hpi
806 [81]. The 35-40 hpi timepoint was included at Generation 1 to account for potential delayed
807 stage development in mutant HBB genotypes (see section on "Red blood cells with mutant
808 HBB genotypes delay parasite development"). Four independent experiments were conducted,
809 with RBC samples included in each experiment detailed in S10 Table. Each experiment

810 included a fresh HbAA blood sample to control the effect of RBC storage after
811 cryopreservation.
812 Samples for flow cytometry analysis (using a CytoFLEX LX flow cytometer, Beckman
813 Coulter) were prepared by resuspending parasite cultures (1:3) in PBS containing 1% BSA,
814 followed by staining with Hoechst 33342 (1:500, BD Pharmingen) in a final volume of 100 µl
815 per well. Samples were then incubated at 37°C for 30 minutes. To measure parasitemia and
816 proportion of schizont stages, flow cytometry analysis (with 100,000 events collected per
817 sample) was set to detect Hoechst 33342 (350 nm laser; 450/40 filter). RBCs were gated by
818 plotting side scatter area (SSC-A) versus forward scatter area (FSC-A), with singlets selected
819 using FSC-H versus FSC-A. Parasites were identified within the singlet gate by Hoechst
820 fluorescence. Hoechst-positive events were defined as exceeding background levels from
821 unstained negative controls. To quantify SCRs, Hoechst fluorescence was combined with the
822 fluorescent reporter TdTom (561 nm laser; 610/20 filter) that is integrated in the NF54-*gexp02-*
823 *Tom* line to distinguish sexual (Hoechst+/tdTom+) from asexual (Hoechst+/tdTom-) parasites.
824 SCRs were calculated as the proportion of Hoechst+/tdTom+ events among all Hoechst+
825 events.
826 SCRs were expressed as a percentage (median [IQR]) per HBB genotype (Figs 3B and S3A-
827 C). Fold-changes in SCRs for HbAC, HbAS, HbSS and HbSC were calculated relative to
828 HbAA by dividing median SCR of each mutant genotype group by that of the wild-type HbAA
829 group. Statistical analysis was performed as described in the section on ”Data analysis”, to
830 assess differences in SCRs (Figs 3B and S3A-C) and potential confounding effect of post-
831 sorbitol initial parasitemia (S1B Fig) across HBB genotypes. Reticulocyte percentages were
832 measured for all RBC samples on the same day as Percoll synchronization (Generation -1, Fig
833 3A). Briefly, RBC suspensions were mixed 1:1 with reticulocyte stain (Sigma-Aldrich),
834 incubated 15 min at room temperature, and used to prepare a thin blood smear for LM

835 estimation of reticulocyte percentage. We determined the ABO and Rhesus D blood groups in
836 all samples using agglutination tests with Seraclone™ Anti-A, Anti-B, and Anti-D (RH1)
837 reagents (Bio-Rad).

838 Parasite development in red blood cells with different HBB 839 genotypes

840 Parasite stage development was evaluated during the *iv*SCAs (Fig 3A) at 35-40 hpi (Generation
841 0) and 25-30 hpi/35-40 hpi (Generation 1) using LM and flow cytometry. The proportion of
842 rings, trophozoites and early/late schizonts was quantified at 35-40 hpi in Generation 0 and 25-
843 30 hpi/35-40 hpi in Generation 1 by LM of Giemsa-stained thin blood smears (100 parasite
844 counts per sample; Fig 4A) in a subset of RBC samples (HbAA n = 1; HbAC n = 1; HbAS n =
845 2; HbSS n = 2; HbSC n = 2). Flow cytometry was used as described earlier to determine the
846 percentage of late stages. For this a distinct population of cells were gated with increased
847 Hoechst 33342 fluorescence (increased DNA content due to multiplication of the nuclei in
848 schizont stages), within the Hoechst+ cells (Fig 4B). Upon confirming consistent results
849 between LM and flow cytometry after screening the same samples by flow cytometry, the same
850 technique was subsequently used in all *iv*SCA samples (HbAA n = 5, HbAC n = 5 and HbAS
851 n = 4, and HbSC n = 1 donors from a malaria-endemic area in Nanoro, Burkina Faso; HbSS n
852 = 12, HbSC n = 1 and n = 6 control HbAA donors [HbAA CTRL] from a non-endemic area)
853 to determine the proportion of late-stages (*i.e.,* schizonts) by HBB genotype (Figs 4B and 4C).
854 From LM data we calculated: (1) the percentage of rings, trophozoites and early/late schizonts
855 (Fig 4A), (2) the mean parasite age using the age in hpi [116] of each stage (rings, trophozoites,
856 schizonts) and the observed proportions; and (3) the developmental delay (in hours) by
857 subtracting mean parasite age of the mutant genotypes from the wild-type HbAA genotype.
858 Finally, for each genotype, we compared the developmental delay between Generations 0 and

859 1 by calculating the difference in mean parasite age at 35-40 hpi between both generations.
860 Then, the development of each independent NF54-*gexp02-Tom* culture was classified as:
861 *expected development*, *delayed development* or *(partially) arrested/extremely delayed*
862 *development* (see detailed analysis in *S1 Appendix)*.

863 IgG and IgM detection by flow cytometry against *Plasmodium*
864 *falciparum*

865 To study the IgG and IgM reactivity against *P. falciparum* in individuals with different HBB
866 genotypes by flow cytometry, we selected plasma samples from humans living in a malaria-
867 endemic area from the *InHost* longitudinal cohort study [74]. We classified samples as
868 "endemic" (endemic plasma) or "non-endemic" (non-endemic plasma) for malaria based on
869 the country of origin. An "endemic" country has consistent, stable *P. falciparum* transmission,
870 while a "non-endemic" country has no local transmission, with infections typically imported
871 [117]. As the expected variation and magnitude of potential differences among HBB genotypes
872 were unknown, we based the sample size on the minimum of 8 individuals per HBB genotype
873 used in the *ev*SCAs and *iv*SCAs. A maximum of 15-20 individuals per genotype was included
874 to ensure sufficient sampling. Selection criteria included equal representation of the most
875 frequent genotype groups (HbAA [n = 18], HbAC [n = 18], HbAS [n = 18], HbCC [n = 2], and
876 HbSC [n = 5]), *P. falciparum* infection status with a large proportion of active *P. falciparum*
877 infections (n = 10-15) and a smaller proportion of non-infected individuals (n = 2-5), age range
878 (1-19 years to exclude maternal antibodies), and homogeneous distribution amongst the
879 ethnicity (all Mossi) and village (Nanoro, Nazoanga, Soum, and Séguédin) groups. Table 2
880 shows the number of participants per HBB genotype included in the assays. The *P. falciparum*
881 transgenic line NF54-*gexp02*-Tom [65, 81] was cultured under the same conditions as
882 described in the *iv*SCAs section and Fig 3A, with the following modifications: (1) parasites

883 were cultured only in wild-type HbAA fresh RBCs and (2) flow cytometry assays were
884 performed on early trophozoite/stage I gametocyte-iRBCs at 20-25 hpi (Generation 1),
885 following the protocol reported in Dantzler KW., et al., (2019) [82] with the adaptations
886 described below.
887 Human plasma samples were pre-diluted in PBS with 1% Bovine Serum Albumin (BSA, Sigma
888 Aldrich) and heparin (2,500U; Sigma Aldrich) (PBS-BSA-Hep) at dilutions of 1:5000 (IgG)
889 and 1:100 (IgM). *In vitro* generated trophozoite- and stage I gametocyte-iRBCs (25-30hpi;
890 Generation 1) were pre-diluted to 0.6% Hct in PBS-BSA-Hep. Pre-diluted human plasma
891 samples were incubated at a 1:10 dilution with pre-diluted trophozoite- and stage I gametocyte-
892 iRBCs, in separate 96-well plates for IgG and IgM assays for 1.5 hours at room temperature.
893 After 2 washes with PBS-BSA-Hep, secondary antibodies were added to the trophozoite- and
894 stage I gametocyte-iRBCs for 30 minutes at 4°C at 0.6% hematocrit. AlexaFluor488 (AF488)
895 mouse anti-human IgG (Jackson ImmunoResearch Europe) and PerCP/Cy5.5® mouse anti-
896 human IgM (Abcam) were used at final dilutions of 1:640 and 1:320 in PBS-BSA-Hep for the
897 IgG and IgM assays, respectively. After 2 washes with PBS-BSA-Hep, the DNA stain
898 Hoechst33342 (BD Pharmingen) was added to the trophozoite- and stage I gametocyte-iRBCs
899 at a final dilution of 1:5000 in PBS-BSA-Hep at 0.6% hematocrit for 30 minutes at 37°C. To
900 verify that the trophozoite- and stage I gametocyte-iRBCs measured contained exclusively
901 RBCs (no white blood cells), each batch pre-diluted trophozoite- and stage I gametocyte-iRBCs
902 (to 0.6% hematocrit in PBS-BSA-Hep) were stained with APC anti-human CD236
903 (Glycophorin C) Recombinant Antibody (Biolegend®) in triplicate at a 1:40 final dilution (S4C
904 Fig). Immunostained samples were analyzed on the flow cytometer CytoFLEX LX (Beckman
905 Coulter), collecting 100,000 cells per culture. We analyzed the median proportions (% cells)
906 of total (trophozoites and stage I gametocytes), asexual (trophozoites) and sexual (stage I
907 gametocytes) iRBCs that were positive for IgG and IgM binding to surface antigens on iRBCs.

908 Samples were considered positive for IgG or IgM if the total iRBC proportions exceeded that
909 of a naïve non-endemic plasma from a volunteer (negative control with HbAA genotype with
910 no prior *P. falciparum* infection, from a non-endemic country [*i.e.,* Belgium] collected at the
911 clinic of the Institute of Tropical Medicine [ITM] in Antwerp). Three non-endemic samples
912 from an acute *P. falciparum*-infected traveler collected at the ITM clinic at days 0, 21 and 23
913 of *P. falciparum* diagnosis (*i.e.,* acute *P. falciparum-infected* non-endemic plasma D0, D21
914 and D23) were used as positive controls. A schematic of the gating strategy to measure the
915 surface reactivity of asexual (tdTom-) and sexual (tdTom+) iRBCs (Hoechst33342+) to IgG
916 (IgG-positive trophozoite-iRBCs: Hoechst33342+/tdTom-/AF488+ and IgG-positive stage I
917 gametocyte-iRBCs: Hoechst33342+/tdTom+/AF488+) or IgM (IgM-positive trophozoite-
918 iRBCs: Hoechst33342+/tdTom-/PerCP-Cy5.5.+ and IgM-positive stage I gametocyte-iRBCs
919 (Hoechst33342+/ tdTom+/PerCP-Cy5.5.+) in the analyzed endemic human plasma samples is
920 represented in Figs S4B and S4C.
921 To determine the optimal plasma dilution factor, a pool of five endemic and hyperimmune
922 plasma samples from *P. falciparum*-infected individuals in a sub-cohort within the *InHost*
923 study [74] (*i.e., P. falciparum*-infected hyperimmune endemic plasma pool of symptomatic
924 individuals with high *P. falciparum* parasitemia ranging from 45,667 to 175,000 parasites per
925 µl) [66] was titrated for the IgG and IgM assay separately. For the IgM assay, four additional
926 plasma samples were titrated (*i.e.,* "naïve non-endemic plasma" and "acute *P. falciparum*-
927 infected non-endemic plasma at D0, D21 and D23") (S4A Fig).
928 During flow cytometry analysis, the IgG- (Hoechst33342+/tdTom-/+/AF488+) and IgM-
929 positive (Hoechst33342+/tdTom-/+/PerCP-Cy5.5.+) total iRBC proportions for each sample
930 were expressed as total event counts, percentage of positive cells, and median fluorescence
931 intensity (MFI) per HBB genotype group. The IgG- and IgM-positive iRBC proportions and
932 signal were compared by HBB genotype group for the total (trophozoites and stage I

933 gametocytes), asexual (trophozoites) and sexual (stage I gametocytes) iRBCs (Figs 5 and S5).
934 To correct for the background signal from the non-iRBCs in the IgG and the IgM channel, the
935 MFI of all samples (including the positive and the negative controls) was expressed as a ΔMFI.
936 For the asexual and sexual iRBCs, ΔMFI was calculated as ΔMFI (AF488+/PerCP-Cy5.5.+) =
937 ("MFI IgG+/IgM+ of asexual [tdTom-]/sexual [tdTom+] trophozoite-iRBCs
938 [Hoechst33342+]") - ("MFI IgG+/IgM+ of non-iRBCs [tdTom-/Hoechst 33342-]") within each
939 plasma sample. For the total iRBCs, ΔMFI was calculated as ΔMFI (AF488+/PerCP-Cy5.5.+)
940 = ("MFI IgG+ or IgM+ iRBCs [Hoechst33342+]") - ("MFI IgG+ or IgM+ of non-iRBCs
941 [Hoechst33342-]" of trophozoite stages incubated with PBS-BSA-Hep, instead of plasma).

942 Data analysis

943 All flow cytometry data were analyzed using FlowLogic™ version 8.7 (Inivai
944 Technologies™). Statistical analyses were performed in R version >4.5.1 (R Core Team 2025),
945 RStudio software version 2025.09.1+401(©2025 Posit Software; RRID:SCR_000432) and the
946 following R packages: brms v. 2.23.0 [118-120], DHARMa v. 0.4.7 [121], emmeans v. 1.11.2.8
947 [122],ggplot2 v.4.00 [123], glmmTMB v. 1.1.13 [124, 125], here v. 1.0.2 [126], lme4 v. 1.1.37
948 [127], performance v. 0.15.2 [128], renv v. 1.1.5 [129], rmarkdown v. 2.30 [130-132], scales
949 v. 1.4.0 [133], sjPlot v. 2.9.0 [134], tidyverse v. 2.0.0 [135], with p-values ($p < 0.05$) considered
950 significant.
951 Risk analysis was conducted to examine associations of demographic and clinical variables
952 (*e.g.,* gender, age, village, ethnicity) across HBB genotype groups (S2, S4 and S8 Tables for
953 the *ev*SCAs, *iv*SCAs, and IgG and IgM detection, respectively). An additional risk analysis for
954 factors associated with elevated SCRs included the same covariates with the addition of HBB
955 genotype (Table 1, for the *iv*SCAs). Continuous variables were analyzed using the Kruskal-
956 Wallis test when parametric assumptions were not met, and when significant, this was followed

957 by Wilcoxon rank sum post-hoc tests for pairwise comparisons with Holm correction.
958 Otherwise, One-way ANOVA or Welch's ANOVA was applied depending on whether
959 Bartlett's test indicated equal or unequal variances, respectively. When significant, Bonferroni-
960 corrected post-hoc pairwise comparisons were performed. Associations between categorical
961 variables were evaluated using Fisher's exact test. Spearman correlation was used for
962 correlation between continuous variables with no normal distribution.

963 For modelling SCR, parasite stage proportions, initial parasitemia and reticulocyte proportions
964 in *ev*SCAs, and *iv*SCAs, and IgG/IgM proportions in the flow cytometry assays, the statistical
965 analysis type was chosen based on the nature of the variables: proportions based on counts
966 were assessed using beta-binomial generalized linear models (GLM) and mixed models
967 (GLMM) with Bonferroni adjustment for the odds ratio contrasts in pairwise comparisons. We
968 chose beta-binomial models due to (possible) violations of the assumptions of the binomial
969 model (namely overdispersion). For *ev*SCA, random factors were used to account for technical
970 replicates and a per-HBB-genotype dispersion factor was added to the GLMM model to
971 account for heteroskedasticity. To address the liberal parametric Wald Z estimates and
972 confidence intervals (asymptotic approximations) provided by the Generalized linear (mixed)
973 models [GL(M)M models], we also computed more conservative Bayesian estimates, odds
974 ratios and credible intervals using a Markov chain Monte Carlo (MCMC) approach when
975 model specification and convergence allowed. GLM and GLMM model specifications and
976 analysis results are reported in S1A-C Table. When the assumptions of the parametric beta-
977 binomial models were violated (*e.g.,* dispersion or quantile deviations as assessed by
978 DHARMa), we instead performed non-parametric Kruskal-Wallis and pairwise Wilcoxon
979 rank-sum tests as described below.

980 Variable selection was guided by a focus on the primary biological variable of interest while
981 avoiding model overspecification and multicollinearity, given the small sample size and

982 unbalanced group structure in terms of potential confounding factors. Our primary analyses
983 therefore focused on the association between SCR, HBB genotype, parasite stages, parasitemia
984 and reticulocyte proportions.

985 For each analysis, we considered additional demographic and clinical variables as potential
986 confounders. Univariate risk analysis of the *iv*SCA data suggested possible associations
987 between SCR and other variables (Table S4). Originally correcting for confounding factors was
988 not part of the experimental design and sample size calculations which resulted in low number
989 of observations per level and sparse and uneven representation in the *iv*SCA. Consequently we
990 were unable to properly control for those variables in the GL(M)M analyses (or without
991 violating modelling assumptions in the case of *ev*SCA), Moreover, likelihood ratio tests did
992 not indicate improved model fit when additional variables were included, compared to models
993 using HBB genotype as the sole independent variable. We therefore focused on a descriptive
994 modelling approach and prioritized parsimonious models with a single parameter of interest,
995 which provided the most interpretable inference given the constraints posed by the available
996 data.

997 Although this approach cannot fully exclude confounding or interaction effects, the direction
998 and magnitude of estimated effects were broadly consistent across alternative model
999 specifications. Sample size and power limitations should still be kept in mind when interpreting
1000 some of these GL(M)M results, with emphasis on effect sizes over exact p-values.

1001 Ethical approvals

1002 The *InHost* study, a longitudinal cohort in Burkina Faso, was approved by the ethical review
1003 board of the Comité d'Éthique pour la Recherche en Santé (CERS: 2018/10/131) in Burkina
1004 Faso, and by the IRB-ITM (1261/18) and IRB-UZA (19/06/064) in Belgium. The amendment

1005 for our nested study in the *InHost* study was approved by CERS (N°2022000140/MSHP/
1006 MESRI/CERS), the IRB at ITM (1261/18), and the IRB at UZA (3347) in Belgium. Ethical
1007 approval for additional sample collection at the Hematology Unit at UZA was granted by the
1008 IRBs at ITM (1538/21) and UZA (3215).

1009 ACKNOWLEDGEMENTS

1010 We are grateful to Robert W Sauerwein and Teun Bousema (Radboud University, The
1011 Netherlands) for the anti-Pfs16 monoclonal antibody. We thank Núria Casas-Vila (ISGlobal)
1012 for the support and guidance in setting up the *ex vivo* and *in vitro* SC assays. We thank Eduard
1013 Rovira-Vallbona (ISGlobal) for helpful discussions on hemoglobin beta variants and aspects
1014 of the *in vitro* study.

1015 REFERENCES

1016 1. WHO. World malaria report 2025: *Addressing the threat of antimalarial drug*
1017 *resistance*. Geneva: 2025
1018 2. Hannemann A WE, Rees DC, Dalibalta S, Ellory JC, Gibson JS. The Properties of
1019 Red Blood Cells from Patients Heterozygous for HbS and HbC (HbSC Genotype). Anemia.
1020 2011;2011:248527 doi: 10.1155/2011/248527.
1021 3. Haldane JB. Suggestions as to quantitative measurement of rates of evolution.
1022 Evolution. 1949;3(1):51-6. doi: 10.1111/j.1558-5646.1949.tb00004.x.
1023 4. Taylor SC, CC; Fairhurst, RM. Hemoglobinopathies: slicing the Gordian knot of
1024 *Plasmodium falciparum* malaria pathogenesis. PLoS Pathog. 2013;9(5):e1003327. doi:
1025 10.1371/journal.ppat.1003327.
1026 5. Taylor S PC, Fairhurst R. Haemoglobinopathies and the clinical epidemiology of
1027 malaria: A systematic review and meta-analysis. Lancet Infect Dis. 2012;12(6):457-68. doi:
1028 10.1016/S1473-3099(12)70055-5.
1029 6. MJ. F. Erythrocytic mechanism of sickle cell resistance to malaria. Proc Natl Acad Sci
1030 USA. 1978;75(4):1994-7. doi: 10.1073/pnas.75.4.1994.
1031 7. Agarwal A, Guindo, A., Cissoko, Y., Taylor, J. G., Coulibaly, D., Koné, A., et al.
1032 Hemoglobin C associated with protection from severe malaria in the Dogon of Mali, a West
1033 African population with a low prevalence of hemoglobin S. Blood. 2000;96(7):2358–63. doi:
1034 10.1182/blood.V96.7.2358.
1035 8. Modiano D LG, Sirima BS, Simporé J, Verra F, Konaté A, Rastrelli E, et al.
1036 Haemoglobin C protects against clinical Plasmodium falciparum malaria. Nature.
1037 2001;414(6861):305–8. doi: 10.1038/35104556
1038 9. Mackinnon MJ MT, Snow RW, Marsh K, Williams TN. Heritability of malaria in
1039 Africa. PLoS Med. 2005;2(12):e340. doi: 10.1371/journal.pmed.0020340.

10. de Mendonça VR GM, Barral-Netto M. The host genetic diversity in malaria infection. J Trop Med. 2012;2012:940616. doi: 10.1155/2012/940616.
11. Lawrence C FM, Nagel RL. The unique red cell heterogeneity of SC disease: crystal formation, dense reticulocytes, and unusual morphology. Blood. 1991;78(8):2104–12. doi: 10.1182/blood.V78.8.2104.2104.
12. Rees DC WT, Gladwin MT. Sickle-cell disease. Lancet. 2010;376(9757):2018-31. doi: 10.1016/S0140-6736(10)61029-X.
13. Grosse SD OI, Atrash HK, Amendah DD, Piel FB, Williams TN. Sickle cell disease in Africa: a neglected cause of early childhood mortality. Am J Prev Med. 2011;41(6 Suppl 4):S398–S405. doi: 10.1016/j.amepre.2011.09.013.
14. Bunn HF NC, Hofrichter J, Schechter GP, Schechter AN, Eaton WA. Molecular and cellular pathogenesis of hemoglobin SC disease. Proc Natl Acad Sci USA. 1982;79(23):7527–31. doi: 10.1073/pnas.79.23.7527.
15. Karna B JS, Al Zaabi E. Hemoglobin C Disease: Treasure Island (FL): StatPearls Publishing; 2025 [updated 2023 May 29].
16. Ballas SK LC, Noone AM, Krasnow SH, Kamarulzaman E, Burka ER. Clinical, hematological, and biochemical features of Hb SC disease. Am J Hematol. 1982;13(1):37-51. doi: 10.1002/ajh.2830130106.
17. Wellems TE, Fairhurst RM. Malaria-protective traits at odds in Africa? Nat Genet. 2005;37(11):1160-2. doi: 10.1038/ng1105-1160.
18. Natama HM, Rovira-Vallbona E, Krit M, Guetens P, Sorgho H, Somé MA, et al. Genetic variation in the immune system and malaria susceptibility in infants: a nested case-control study in Nanoro, Burkina Faso. Malar J. 2021;20(1)(1475-2875):94. doi: 10.1186/s12936-021-03628-y.
19. Simpore J, Pignatelli, S., Barlati, S., & Musumeci, S. Modification in the frequency of Hb C and Hb S in Burkina Faso: an influence of migratory fluxes and improvement of patient health care. Hemoglobin. 2002;26(2):113–20. doi: 10.1081/hem-120005448.
20. Bougouma EC, Tiono AB, Ouédraogo A, Soulama I, Diarra A, Yaro J-B, et al. Haemoglobin variants and Plasmodium falciparum malaria in children under five years of age living in a high and seasonal malaria transmission area of Burkina Faso. Malar J. 2012;11(1):154. doi: 10.1186/1475-2875-11-154.
21. May J, Evans, J. A., Timmann, C., Ehmen, C., Busch, W., Thye, T., et al. Hemoglobin variants and disease manifestations in severe falciparum malaria. JAMA. 2007;297(20):2220–6. doi: 10.1001/jama.297.20.2220.
22. Williams TN MT, Roberts DJ, Alexander ND, Weatherall DJ, Wambua S, et al. . An immune basis for malaria protection by the sickle cell trait. PLoS Med. 2005;2(5):e128. doi: 10.1371/journal.pmed.0020128.
23. Williams TN, Mwangi, T. W., Wambua, S., Alexander, N. D., Kortok, M., Snow, R. W., et al. . Sickle cell trait and the risk of Plasmodium falciparum malaria and other childhood diseases. J Infect Dis. 2005;192(1):178–86. doi: 10.1086/430744.
24. Gong L, Parikh S, Rosenthal PJ, Greenhouse B. Biochemical and immunological mechanisms by which sickle cell trait protects against malaria. Malar J. 2013;12(1):317. doi: 10.1186/1475-2875-12-317.
25. Archer NM, Petersen N, Clark MA, Buckee CO, Childs LM, Duraisingh MT. Resistance to Plasmodium falciparum in sickle cell trait erythrocytes is driven by oxygen-dependent growth inhibition. Proc Natl Acad Sci USA. 2018;115(28):7350-5. doi: 10.1073/pnas.1804388115.
26. Kaur J, Hora R. '2TM proteins': an antigenically diverse superfamily with variable functions and export pathways. PeerJ. 2018;6:e4757. doi: 10.7717/peerj.4757.

1089 27. Chen S-Y, Wang Y, Telen MJ, Chi J-T. The Genomic Analysis of Erythrocyte
1090 microRNA Expression in Sickle Cell Diseases. PLoS One. 2008;3(6):e2360. doi:
1091 10.1371/journal.pone.0002360.
1092 28. Fairhurst RM, Baruch, D. I., Brittain, N. J., Ostera, G. R., Wallach, J. S., Hoang, H.
1093 L., et al. . Abnormal display of PfEMP-1 on erythrocytes carrying haemoglobin C may
1094 protect against malaria. Nature. 2005;435(7045):1117–21. doi: 10.1038/nature03631.
1095 29. Gong L M-SC, Rosenthal PJ, Hubbard AE, Drakeley CJ, Dorsey G, Greenhouse B.
1096 Evidence for both innate and acquired mechanisms of protection from Plasmodium
1097 falciparum in children with sickle cell trait. Blood. 2012;119(16):3808–14. doi:
1098 10.1182/blood-2011-08-371062.
1099 30. Lelliott PM MB, Foote SJ, Burgio G. The influence of host genetics on erythrocytes
1100 and malaria infection: is there therapeutic potential? Malar J. 2015;14:289. doi:
1101 10.1186/s12936-015-0809-x.
1102 31. Fairhurst RM, Bess CD, Krause MA. Abnormal PfEMP1/knob display on
1103 Plasmodium falciparum-infected erythrocytes containing hemoglobin variants: fresh insights
1104 into malaria pathogenesis and protection. Microbes Infect. 2012;14(10):851-62. doi:
1105 10.1016/j.micinf.2012.05.006.
1106 32. Flage B, Dent MR, Tejero J, Amoah LE, Ofori-Acquah SF. Heme promotes sexual
1107 conversion of Plasmodium falciparum in human erythrocytes. Front Malar. 2023;Volume 1 -
1108 2023. doi: 10.3389/fmala.2023.1161750.
1109 33. Vasquez M, Zuniga M, Rodriguez A. Oxidative Stress and Pathogenesis in Malaria.
1110 Front Cell Infect Microbiol. 2021;11(2235-2988):768182. doi: 10.3389/fcimb.2021.768182.
1111 34. Cyrklaff M, Sanchez CP, Kilian N, Bisseye C, Simpore J, Frischknecht F, et al.
1112 Hemoglobins S and C interfere with actin remodeling in Plasmodium falciparum-infected
1113 erythrocytes. Science. 2011;334(6060):1283-6. doi: 10.1126/science.1213775.
1114 35. Cholera R, Brittain, N. J., Gillrie, M. R., Lopera-Mesa, T. M., Diakité, S. A., Arie, T.,
1115 et al. Impaired cytoadherence of Plasmodium falciparum-infected erythrocytes containing
1116 sickle hemoglobin. Proc Natl Acad Sci USA. 2008;105(3)(1091-6490 (Electronic)):991–6.
1117 doi: 10.1073/pnas.0711401105.
1118 36. Gouagna LC, Bancone G, Yao F, Yameogo B, Dabire KR, Costantini C, et al. Genetic
1119 variation in human HBB is associated with Plasmodium falciparum transmission. Nat Genet.
1120 2010;42(4):328-31. doi: 10.1038/ng.554.
1121 37. Gonçalves BP, Sagara I, Coulibaly M, Wu Y, Assadou MH, Guindo A, et al.
1122 Hemoglobin variants shape the distribution of malaria parasites in human populations and
1123 their transmission potential. Sci Rep. 2017;7(1):14267-. doi: 10.1038/s41598-017-14627-y.
1124 38. Andolina C, Ramjith J, Rek J, Lanke K, Okoth J, Grignard L, et al. Plasmodium
1125 falciparum gametocyte carriage in longitudinally monitored incident infections is associated
1126 with duration of infection and human host factors. Sci Rep. 2023;13(1):7072. doi:
1127 10.1038/s41598-023-33657-3.
1128 39. Lawaly YR, Sakuntabhai A, Marrama L, Konate L, Phimpraphi W, Sokhna C, et al.
1129 Heritability of the human infectious reservoir of malaria parasites. PLoS One.
1130 2010;5(6):e11358-e. doi: 10.1371/journal.pone.0011358.
1131 40. Ngou CM, Bayibéki AN, Abate L, Makinde OS, Feufack-Donfack LB, Sarah-Matio
1132 EM, et al. Influence of the sickle cell trait on Plasmodium falciparum infectivity from
1133 naturally infected gametocyte carriers. BMC Infect Dis. 2023;23(1):317. doi:
1134 10.1186/s12879-023-08134-x.
1135 41. Meibalan EM, M. Biology of Malaria Transmission. Cold Spring Harb Perspect Med.
1136 2017;7(3):a025452. doi: 10.1101/cshperspect.a025452.

1137 42. Bousema T, Drakeley C. Epidemiology and infectivity of Plasmodium falciparum and
1138 Plasmodium vivax gametocytes in relation to malaria control and elimination. Clin Microbiol
1139 Rev. 2011;24(2):377-410. doi: 10.1128/cmr.00051-10.
1140 43. Ngotho P, Soares AB, Hentzschel F, Achcar F, Bertuccini L, Marti M. Revisiting
1141 gametocyte biology in malaria parasites. FEMS Microbiol Rev. 2019;43(4):401-14. doi:
1142 10.1093/femsre/fuz010.
1143 44. Llorà-Batlle O, Michel-Todó L, Witmer K, Toda H, Fernández-Becerra C, Baum J, et
1144 al. Conditional expression of PfAP2-G for controlled massive sexual conversion in
1145 Plasmodium falciparum. Sci Adv. 2020;6(24):eaaz5057. doi: 10.1126/sciadv.aaz5057.
1146 45. Bancells C, Llora-Batlle O, Poran A, Notzel C, Rovira-Graells N, Elemento O, et al.
1147 Revisiting the initial steps of sexual development in the malaria parasite *Plasmodium*
1148 *falciparum*. Nat Microbiol. 2019;4(1):144-54. doi: 10.1038/s41564-018-0291-7.
1149 46. Kafsack BF, Rovira-Graells N, Clark TG, Bancells C, Crowley VM, Campino SG, et
1150 al. A transcriptional switch underlies commitment to sexual development in malaria parasites.
1151 Nature. 2014;507(7491):248-52. doi: 10.1038/nature12920.
1152 47. Brancucci NMB BN, Zhu L, Niederwieser I, Chin WH, Wampfler R, et al.
1153 Heterochromatin protein 1 secures survival and transmission of malaria parasites. Cell Host
1154 Microbe. 2014;16(2):165-76. doi: 10.1016/j.chom.2014.07.004.
1155 48. Farid R, Dixon MW, Tilley L, McCarthy JS. Initiation of gametocytogenesis at very
1156 low parasite density in Plasmodium falciparum infection. J Infect Dis. 2017;215(7):1167-74.
1157 doi: 10.1093/infdis/jix035.
1158 49. Usui M, Prajapati SK, Ayanful-Torgby R, Acquah FK, Cudjoe E, Kakaney C, et al.
1159 Plasmodium falciparum sexual differentiation in malaria patients is associated with host
1160 factors and GDV1-dependent genes. Nat Commun. 2019;10(1):2140. doi: 10.1038/s41467-
1161 019-10172-6.
1162 50. Pelle KG, Oh K, Buchholz K, Narasimhan V, Joice R, Milner DA, et al.
1163 Transcriptional profiling defines dynamics of parasite tissue sequestration during malaria
1164 infection. Genome Med. 2015;7(1):19. doi: 10.1186/s13073-015-0133-7.
1165 51. Prajapati SK, Ayanful-Torgby R, Pava Z, Barbeau MC, Acquah FK, Cudjoe E, et al.
1166 The transcriptome of circulating sexually committed Plasmodium falciparum ring stage
1167 parasites forecasts malaria transmission potential. Nat Commun. 2020;11(1):6159. doi:
1168 10.1038/s41467-020-19988-z.
1169 52. Venugopal K HF, Valkiūnas G, Marti M. Plasmodium asexual growth and sexual
1170 development in the haematopoietic niche of the host. Nat Rev Microbiol. 2020;18(3):177–89.
1171 doi: 10.1038/s41579-019-0306-2.
1172 53. Churcher TS BT, Walker M, Drakeley C, Schneider P, Ouédraogo AL, Basáñez MG.
1173 Predicting mosquito infection from Plasmodium falciparum gametocyte density and
1174 estimating the reservoir of infection. eLife. 2013;2:e00626. doi: 10.7554/eLife.00626.
1175 54. Bousema T, Drakeley C. Determinants of Malaria Transmission at the Population
1176 Level. . Cold Spring Harb Perspect Med. 2017;7(12):a025510. doi:
1177 10.1101/cshperspect.a025510.
1178 55. Bradley J, Stone W, Da DF, Morlais I, Dicko A, Cohuet A, et al. Predicting the
1179 likelihood and intensity of mosquito infection from sex specific Plasmodium falciparum
1180 gametocyte density. eLife. 2018;7:e34463. doi: 10.7554/eLife.34463.
1181 56. Barry A, Bradley J, Stone W, Guelbeogo MW, Lanke K, Ouedraogo A, et al. Higher
1182 gametocyte production and mosquito infectivity in chronic compared to incident Plasmodium
1183 falciparum infections. Nat Commun. 2021;12(1):2443. doi: 10.1038/s41467-021-22573-7.
1184 57. Barry A. Mosquitoes infecting children & children infecting mosquitoes in Burkina
1185 Faso: Production and infectivity of malaria transmission stages (Doctoral dissertation).
1186 Radboud Universiteit Nijmegen: Radboud Universiteit Nijmegen; 2022.

58. Ahmad A, Soumare HM, Camara MM, Jadama L, Gaye PM, Bittaye H, et al. Infectivity of patent Plasmodium falciparum gametocyte carriers to mosquitoes: establishing capacity to investigate the infectious reservoir of malaria in a low-transmission setting in The Gambia. Trans R Soc Trop Med Hyg. 2021;115(12):1462–7. doi: 10.1093/trstmh/trab087.
59. Josling GA, Williamson KC, Llinás M. Regulation of Sexual Commitment and Gametocytogenesis in Malaria Parasites. Annu Rev Microbiol. 2018;72:501–19. doi: 10.1146/annurev-micro-090817-062712.
60. Brancucci NMB, Gerdt JP, Wang C, De Niz M, Philip N, Adapa SR, et al. Lysophosphatidylcholine Regulates Sexual Stage Differentiation in the Human Malaria Parasite Plasmodium falciparum. Cell. 2017;171(7):1532-44.e15. doi: 10.1016/j.cell.2017.10.020.
61. Neveu G, Beri D, Kafsack BF. Metabolic regulation of sexual commitment in Plasmodium falciparum. Curr Opin Microbiol. 2020;58:93–8. doi: 10.1016/j.mib.2020.09.004.
62. Harris CT TX, Campelo R, Marreiros IM, Vanheer LN, Nahiyaan N, et al. Sexual differentiation in human malaria parasites is regulated by competition between phospholipid metabolism and histone methylation. Nat Microbiol. 2023;8(7):1280–92. doi: 10.1038/s41564-023-01396-w.
63. Trager W, Gill GS, Lawrence C, Nagel RL. Plasmodium falciparum: enhanced gametocyte formation in vitro in reticulocyte-rich blood. Exp Parasitol. 1999;91(2):115-8. doi: 10.1006/expr.1998.4347.
64. Birget PLG, Repton C, O'Donnell AJ, Schneider P, Reece SE. Phenotypic plasticity in reproductive effort: malaria parasites respond to resource availability. Proc Biol Sci. 2017;284(1860):20171229. doi: 10.1098/rspb.2017.1229.
65. Portugaliza HP, Miyazaki S, Geurten FJA, Pell C, Rosanas-Urgell A, Janse CJ, et al. Artemisinin exposure at the ring or trophozoite stage impacts Plasmodium falciparum sexual conversion differently. eLife. 2020;9:e60058. doi: 10.7554/eLife.60058.
66. Portugaliza HP, Natama HM, Guetens P, Rovira-Vallbona E, Somé AM, Millogo A, et al. Plasmodium falciparum sexual conversion rates can be affected by artemisinin-based treatment in naturally infected malaria patients. EBioMedicine. 2022;83:104198. doi: 10.1016/j.ebiom.2022.104198.
67. Thommen BT, Passecker A, Buser T, Hitz E, Voss TS, Brancucci NMB. Revisiting the Effect of Pharmaceuticals on Transmission Stage Formation in the Malaria Parasite Plasmodium falciparum. Front Cell Infect Microbiol. 2022;12:802341. doi: 10.3389/fcimb.2022.802341.
68. Peatey CL, Skinner-Adams, T. S., Dixon, M. W., McCarthy, J. S., Gardiner, D. L., & Trenholme, K. R. Effect of antimalarial drugs on Plasmodium falciparum gametocytes. . J Infect Dis. 2009;200(10):1518–21. doi: 10.1086/644645.
69. Verra F, Simpore J, Warimwe GM, Tetteh KK, Howard T, Osier FHA, et al. Haemoglobin C and S Role in Acquired Immunity against Plasmodium falciparum Malaria. PLoS One. 2007;2(10):e978. doi: 10.1371/journal.pone.0000978.
70. Diatta AM ML, Tall A, Trape JF, Dieye A, Garraud O, et al. Relationship of binding of immunoglobulin G to Plasmodium falciparum-infected erythrocytes with parasite endemicity and antibody responses to conserved antigen in immune individuals. Clin Diagn Lab Immunol. 2004;11(1):6–11. doi: 10.1128/cdli.11.1.6-11.2004.
71. Cabrera G CM, Migot-Nabias F, Kremsner PG, Deloron P, Luty AJF. The sickle cell trait is associated with enhanced immunoglobulin G antibody responses to Plasmodium falciparum variant surface antigens. J Infect Dis. 2005;191(10):1631–8. doi: 10.1086/429832.

1235 72. Bailey RD, Lawton JG, Niangaly A, Stucke EM, Bailey JA, Berry AA, et al. Children
1236 with hemoglobin C or S trait have low serologic responses to a subset of malaria variant
1237 surface antigens. J Infect. 2024;89(4):106257. doi: 10.1016/j.jinf.2024.106257.
1238 73. Asare KK, Agrah B, Ofori-Acquah FS, Kudzi W, Aryee NA, Amoah LE. Immune
1239 responses to P. falciparum antibodies in symptomatic malaria patients with variant
1240 hemoglobin genotypes in Ghana. BMC Immunol. 2024;25(1):14. doi: 10.1186/s12865-024-
1241 00607-1.
1242 74. Natama HM, Ouédraogo DF, Kuehne V, Guetens P, Millogo A, Moreno-Murillo A, et
1243 al. Plasmodium falciparum infectious reservoir in a rural setting in Burkina Faso: a two-year
1244 cohort study. medRxiv. 2026:2026.01.09.26343521. doi: 10.64898/2026.01.09.26343521.
1245 75. Baker DA-O, Stewart LB, Large JM, Bowyer PW, Ansell KH, Jiménez-Díaz MB, et
1246 al. A potent series targeting the malarial cGMP-dependent protein kinase clears infection and
1247 blocks transmission. Nat Commun. 2017;8(1):430. doi: 10.1038/s41467-017-00572-x.
1248 76. Moelans IIMD. Pfs16, a potential vaccine candidate against the human malaria
1249 parasite *Plasmodium falciparum* (Doctoral dissertation). University of Nijmegen: University
1250 of Nijmegen; 1995.
1251 77. Bruce MC CR, Nakamura K, Aikawa M, Carter R. Cellular location and temporal
1252 expression of the Plasmodium falciparum sexual stage antigen Pfs16. Mol Biochem Parasitol.
1253 1994;65(1):11–22. doi: 10.1016/0166-6851(94)90111-2.
1254 78. Shabani S, Serbus LR. Pfs16: A Key Parasitophorous Vacuole Membrane Protein
1255 Crucial for Malaria Parasite Development and Transmission. Protein J. 2025;44(2)(1875-
1256 8355):133–46. doi: 10.1007/s10930-025-10260-1.
1257 79. Filarsky M, Fraschka SA, Niederwieser I, Brancucci NMB, Carrington E, Carrió E, et
1258 al. GDV1 induces sexual commitment of malaria parasites by antagonizing HP1-dependent
1259 gene silencing. Science. 2018;359(6381):1259-63. doi: 10.1126/science.aan6042.
1260 80. LB. S, Freville A, Voss Till S, Baker David A, Awandare Gordon A, Conway David
1261 J. Plasmodium falciparum Sexual Commitment Rate Variation among Clinical Isolates and
1262 Diverse Laboratory-Adapted Lines. Microbiol Spectr. 2022;10(6):e02234-22. doi:
1263 10.1128/spectrum.02234-22.
1264 81. Portugaliza HP, Llorà-Batlle O, Rosanas-Urgell A, Cortés A. Reporter lines based on
1265 the *gexp02* promoter enable early quantification of sexual conversion rates in the malaria
1266 parasite *Plasmodium falciparum*. Sci Rep. 2019;9(1):14595. doi: 10.1038/s41598-019-50768-
1267 y.
1268 82. Dantzler KW, Ma S, Ngotho P, Stone WJR, Tao D, Rijpma S, et al. Naturally
1269 acquired immunity against immature Plasmodium falciparum gametocytes. Sci Transl Med.
1270 2019;11(495):eaav3963. doi: 10.1126/scitranslmed.aav3963.
1271 83. Boyle MJ, Chan JA, Handayuni I, Reiling L, Feng G, Hilton A, et al. IgM in human
1272 immunity to Plasmodium falciparum malaria. Sci Adv. 2019;5(9):eaax4489. doi:
1273 10.1126/sciadv.aax4489.
1274 84. Walker MR, Knudsen AS, Partey FD, Bassi MR, Frank AM, Castberg FA-O, et al.
1275 Acquisition and decay of IgM and IgG responses to merozoite antigens after Plasmodium
1276 falciparum malaria in Ghanaian children. PLoS One. 2020;15(12): e0243943. doi:
1277 10.1371/journal.pone.0243943.
1278 85. Stanisic DI, Fowkes FJ, Koinari M, Javati S, Lin E, Kiniboro B, et al. Acquisition of
1279 antibodies against Plasmodium falciparum merozoites and malaria immunity in young
1280 children and the influence of age, force of infection, and magnitude of response. Infect
1281 Immun. 2015;83(2):646–60. doi: 10.1128/IAI.02398-14.
1282 86. Rogier E, Nace D, Dimbu PR, Wakeman B, Beeson JG, Drakeley C, et al. Antibody
1283 dynamics in children with first or repeat Plasmodium falciparum infections. Front Med.
1284 2022;9:869028. doi: 10.3389/fmed.2022.869028.

1285 87. Akpogheneta OJ, Duah, N. O., Tetteh, K. K., Dunyo, S., Lanar, D. E., Pinder, M., et
1286 al. Duration of naturally acquired antibody responses to blood-stage Plasmodium falciparum
1287 is age dependent and antigen specific. Infect Immun. 2008;76(4):1748–55. doi:
1288 10.1128/IAI.01333-07.
1289 88. Chelimo K, Ofulla, A. V., Narum, D. L., Kazura, J. W., Lanar, D. E., & John, C. C.
1290 Antibodies to Plasmodium falciparum antigens vary by age and antigen in children in a
1291 malaria-holoendemic area of Kenya. Pediatr Infect Dis J. 2005;24(8):680–4. doi:
1292 10.1097/01.inf.0000172151.28851.fd.
1293 89. Amoah LE, Acquah FK, Nyarko PB, Cudjoe E, Donu D, Ayanful-Torgby R, et al.
1294 Comparative analysis of asexual and sexual stage Plasmodium falciparum development in
1295 different red blood cell types. Malar J. 2020;19(1):200. doi: 10.1186/s12936-020-03275-9.
1296 90. Talman AM PR, Sokhna CS, Domarle O, Ariey F, Trape JF, Robert V. . Influence of
1297 chemotherapy on the Plasmodium gametocyte sex ratio of mice and humans. Am J Trop Med
1298 Hyg. 2004;71(6):739-44.
1299 91. Uneke CJ. Plasmodium falciparum malaria and ABO blood group: is there any
1300 relationship? Parasitol Res. 2007;100(4):759–65. doi: 10.1007/s00436-006-0342-5.
1301 92. Wolofsky KT, Ayi, K., Branch, D. R., Hult, A. K., Olsson, M. L., Liles, W. C., et al. .
1302 ABO blood groups influence macrophage-mediated phagocytosis of Plasmodium falciparum-
1303 infected erythrocytes. PLoS Pathog. 2012;8(10):e1002942. doi:
1304 10.1371/journal.ppat.1002942.
1305 93. Afoakwah R, Aubyn E, Prah J, Nwaefuna EK, Boampong JN. Relative
1306 Susceptibilities of ABO Blood Groups to Plasmodium falciparum Malaria in Ghana. Adv
1307 Hematol. 2016;2016:5368793. doi: 10.1155/2016/5368793.
1308 94. Cserti-Gazdewich C, Musoke C, Dhabangi A, Nakiboneka-Ssenabulya D, Ddungu H,
1309 Nabukeera-Barungi N, et al. ABO In Morbidity and Mortality of Plasmodium falciparum
1310 malaria. Blood. 2010;116(21):666-. doi: 10.1182/blood.V116.21.666.666.
1311 95. Sheng K, Shariff M, Hebbel RP. Comparative Oxidation of Hemoglobins A and S.
1312 Blood. 1998;91(9):3467-70. doi: 10.1182/blood.V91.9.3467.
1313 96. Uzunova VV PW, Galkin O, Vekilov PG. Free heme and the polymerization of sickle
1314 cell hemoglobin. Biophys J. 2010;99(6):1976–85. doi: 10.1016/j.bpj.2010.07.024.
1315 97. Fröhlich B, Jäger J, Lansche C, Sanchez CP, Cyrklaff M, Buchholz B, et al.
1316 Hemoglobin S and C affect biomechanical membrane properties of P. falciparum-infected
1317 erythrocytes. Commun Biol. 2019;2:311. doi: 10.1038/s42003-019-0556-6.
1318 98. Smalley ME, & Brown, J. . Plasmodium falciparum gametocytogenesis stimulated by
1319 lymphocytes and serum from infected Gambian children. Trans R Soc Trop Med Hyg.
1320 1981;75(2):316-7. doi: 10.1016/0035-9203(81)90348-5.
1321 99. Tan X, Traore, B., Kayentao, K., Ongoiba, A., Doumbo, S., Waisberg, M., et al.
1322 Hemoglobin S and C heterozygosity enhances neither the magnitude nor breadth of antibody
1323 responses to a diverse array of Plasmodium falciparum antigens. J Infect Dis.
1324 2011;204(11):1750–61. doi: 10.1093/infdis/jir638.
1325 100. Jensen AR, Adams, Y., & Hviid, L. . Cerebral Plasmodium falciparum malaria: The
1326 role of PfEMP1 in its pathogenesis and immunity, and PfEMP1-based vaccines to prevent it.
1327 Immunol Rev. 2020;293(1):230–52. doi: 10.1111/imr.12807.
1328 101. Smith JD, Chitnis CE, Craig AG, Roberts DJ, Hudson-Taylor DE, Peterson DS, et al.
1329 Switches in expression of plasmodium falciparum var genes correlate with changes in
1330 antigenic and cytoadherent phenotypes of infected erythrocytes. Cell. 1995;82(1):101-10. doi:
1331 10.1016/0092-8674(95)90056-X.
1332 102. Wichers-Misterek JS, Krumkamp R, Held J, von Thien H, Wittmann I, Höppner YD,
1333 et al. The exception that proves the rule: Virulence gene expression at the onset of

Plasmodium falciparum blood stage infections. PLoS Pathog. 2023;19(6):e1011468. doi: 10.1371/journal.ppat.1011468.
103. Ngotho P, Dantzler Press K, Peedell M, Muasya W, Omondi BR, Otoboh SE, et al. Reversible host cell surface remodelling limits immune recognition and maximizes survival of Plasmodium falciparum gametocytes. PLoS Pathog. 2025;21(5):e1013110. doi: 10.1371/journal.ppat.1013110.
104. Bousema T, Roeffen W, Meijerink H, Mwerinde H, Mwakalinga S, van Gemert G-J, et al. The Dynamics of Naturally Acquired Immune Responses to Plasmodium falciparum Sexual Stage Antigens Pfs230 & Pfs48/45 in a Low Endemic Area in Tanzania. PLoS One. 2010;5(11):e14114. doi: 10.1371/journal.pone.0014114.
105. Schneider P, Greischar MA, Birget PLG, Repton C, Mideo N, Reece SE. Adaptive plasticity in the gametocyte conversion rate of malaria parasites. PLoS Pathog. 2018;14(11):e1007371. doi: 10.1371/journal.ppat.1007371.
106. WHO. WHO. Basic malaria microscopy: part I. Learner's guide. 2010.
107. Natama HM, Rovira-Vallbona E, Somé MA, Zango SH, Sorgho H, Guetens P, et al. Malaria incidence and prevalence during the first year of life in Nanoro, Burkina Faso: a birth-cohort study. Malar J. 2018;17(1):163. doi: 10.1186/s12936-018-2315-4.
108. Natama HM, Rovira-Vallbona E, Somé MA, Zango SH, Sorgho H, Guetens P, et al. Malaria incidence and prevalence during the first year of life in Nanoro, Burkina Faso: a birth-cohort study. Malar J. 2018;17(1):163. doi: 10.1186/s12936-018-2315-4.
109. Hofmann N, Mwingira F, Shekalaghe S, Robinson LJ, Mueller I, Felger I. Ultra-sensitive detection of Plasmodium falciparum by amplification of multi-copy subtelomeric targets. PLoS Med. 2015;12(3):e1001788. doi: 10.1371/journal.pmed.1001788.
110. Wittwer CT, Reed GH, Gundry CN, Vandersteen JG, Pryor RJ. High-Resolution Genotyping by Amplicon Melting Analysis Using LCGreen. Clin Chem. 2020;49(6):853-60. doi: 10.1373/49.6.853.
111. MMV, WHO. Methods and techniques for clinical trials on antimalarial drug efficacy: genotyping to identify parasite populations. Amsterdam, The Netherlands.2008.
112. Rasouli Ghahfarokhi SM, Asadi F, Obeidi N. Use of capillary electrophoresis for detection of hemoglobinopathies in individuals referred to health centers in Masjed-Soleiman. Iran J Blood Cancer. 2017;9:89-92.
113. da Guarda CC, Yahouédéhou S, Santiago RP, Neres J, Fernandes CFL, Aleluia MM, et al. Sickle cell disease: A distinction of two most frequent genotypes (HbSS and HbSC). PLoS One. 2020;15(1):e0228399. doi: 10.1371/journal.pone.0228399.
114. Ten Hove D, Jorgensen, T. D., & van der Ark, L. A. Updated guidelines on selecting an intraclass correlation coefficient for interrater reliability, with applications to incomplete observational designs. Psychol Methods. 2024;29:967-79. doi: 10.1037/met0000516.
115. EVIMalaR. Methods in Malaria Research2013.
116. Silamut K PN, Whitty C, Turner GD, Louwrier K, Mai NT, et al. A quantitative analysis of the microvascular sequestration of malaria parasites in the human brain. Am J Pathol. 1999;155(2):395–410. doi: 10.1016/S0002-9440(10)65136-X.
117. WHO. World malaria report 2024. 2024 11 December 2024.
118. Bürkner P-C. brms: An R Package for Bayesian Multilevel Models Using Stan. J Stat Softw. 2017;80(1):1-28. doi: 10.18637/jss.v080.i01.
119. Bürkner P-C. Advanced Bayesian Multilevel Modeling with the R Package brms. RJ. 2018;10(1):395-411. doi: 10.32614/RJ-2018-017.
120. Bürkner P-C. Bayesian Item Response Modeling in R with brms and Stan. J Stat Softw. 2021;100(5):1-54. doi: 10.18637/jss.v100.i05.
121. Hartig F. DHARMa: Residual Diagnostics for Hierarchical (Multi-Level / Mixed) Regression Models2024 2024.

122. Lenth RV. emmeans: Estimated Marginal Means, aka Least-Squares Means2025 2025.
123. Wickham H. ggplot2: Elegant Graphics for Data Analysis: Springer-Verlag New York; 2016.
124. Brooks ME, Kristensen K, Benthem KJv, Magnusson A, Berg CW, Nielsen A, et al. glmmTMB Balances Speed and Flexibility Among Packages for Zero-inflated Generalized Linear Mixed Modeling. RJ. 2017;9(2):378-400. doi: 10.32614/RJ-2017-066.
125. McGillycuddy M, Warton DI, Popovic G, Bolker BM. Parsimoniously Fitting Large Multivariate Random Effects in glmmTMB. J Stat Softw. 2025;112(1):1-19. doi: 10.18637/jss.v112.i01.
126. Müller K. here: A Simpler Way to Find Your Files2025 2025.
127. Bates D, Mächler M, Bolker B, Walker S. Fitting Linear Mixed-Effects Models Using lme4. J Stat Softw. 2015;67(1):1-48. doi: 10.18637/jss.v067.i01.
128. Lüdecke D, Ben-Shachar MS, Patil I, Waggoner P, Makowski D. performance: An R Package for Assessment, Comparison and Testing of Statistical Models. J Open Source Softw. 2021;6(60):3139. doi: 10.21105/joss.03139.
129. Ushey K, Wickham H. renv: Project Environments2025 2025.
130. Xie Y, Allaire JJ, Grolemund G. R Markdown: The Definitive Guide. Boca Raton, Florida: Chapman and Hall/CRC; 2018 2018.
131. Xie Y, Dervieux C, Riederer E. R Markdown Cookbook. Boca Raton, Florida: Chapman and Hall/CRC; 2020 2020.
132. Allaire JJ, Xie Y, Dervieux C, McPherson J, Luraschi J, Ushey K, et al. rmarkdown: Dynamic Documents for R2025 2025.
133. Wickham H, Pedersen TL, Seidel D. scales: Scale Functions for Visualization2025 2025.
134. Lüdecke D. sjPlot: Data Visualization for Statistics in Social Science2025 2025.
135. Wickham H, Averick M, Bryan J, Chang W, McGowan LDA, François R, et al. Welcome to the tidyverse. J Open Source Softw. 2019;4(43):1686. doi: 10.21105/joss.01686.

1414 # SUPPORTING INFORMATION

1415 **S1 Appendix:** Assay optimization and validation of *ex vivo* and *in vitro* SC assays, and
1416 IgG/IgM detection by flow cytometry.

1417 **S1 Fig. Correlation analysis between parasitemia and SC rates (SCRs).** (A) *ev*SCAs and
1418 (B) *iv*SCAs. Data points are colored by HBB genotype. Spearman's rank correlation was used;
1419 non-significant correlations are indicated as ns.

1420 **S2 Fig. Representative flow cytometry plots showing tdTomato and Hoechst33342 signals.**
1421 (A) HbAA fresh blood controls cultured under +Choline and -Choline conditions, with and
1422 without Hoechst33342. (B-C) Parasites cultured in cryopreserved RBCs with different HBB
1423 genotypes under +Choline (B) or -Choline (C) conditions.

1424 **S3 Fig. Effect of HBB genotype on SC in *in vitro* SC assays (*iv*SCAs).** Related to Fig 3.
1425 SCRs were measured by flow cytometry at 25-30 hpi in +Choline and -Choline cultures (A-B)
1426 and at 35-40 hpi in -Choline cultures (C). (D-E) Show the proportions of asexual versus sexual
1427 stages and the correlation between reticulocyte percentage and SCRs. Statistical tests: (B-C)
1428 beta-binomial GLMs with Bonferroni correction; (A) Kruskal-Wallis test; (E) Spearman
1429 correlation.

1430 **S4 Fig. Flow cytometry detection of IgG and IgM responses against *P. falciparum*-iRBCs.**
1431 (A) Plasma titration curves with positive and negative controls. (B-C) Gating strategy for
1432 measuring antibody reactivity to asexual (tdTom-) and sexual (tdTom+) iRBCs and verification
1433 of RBC-only populations using Glycophorin C.

1434 **S5 Fig. IgG- and IgM-mediated responses to *Plasmodium falciparum* trophozoites and**
1435 **stage I gametocytes across HBB genotypes.** (A-D) Event counts and MFI for IgG- and IgM-
1436 positive total, asexual, and sexual iRBCs in plasma from *P. falciparum*-infected and non-
1437 infected individuals. Statistical comparisons were performed with beta-binomial GLMs with
1438 Bonferroni correction.

1439 **S6 Fig. IgG- and IgM-positive total iRBCs in plasma from *P. falciparum*-infected and**
1440 **non-infected individuals.** Median proportions of IgG-positive (A) or IgM-positive (B) total-
1441 iRBCs for *Pf*-infected versus non-infected groups. Statistical comparisons were performed
1442 with beta-binomial GLMs with Bonferroni correction.

1443 **S7 Fig. Flow chart of participant selection in the *ex vivo* and *in vitro* SC assays.** Infection
1444 status determined by RDT, LM, and *var*ATS qPCR. Samples meeting parasitemia and RBC
1445 volume criteria were included in respective assays.

1446 **S8 Fig. Experimental variability of SCR measurements in +Choline cultures, grouped by**
1447 **HBB genotype.** Timepoint of measurement: at 35-40 hpi (Generation 1).

1448 **S1A Table. Statistical analysis outcomes from GLMs or GLMMs and Kruskal-Wallis**
1449 **tests in *ex vivo* SC assays.**

1450 **S1B Table. Statistical analysis outcomes from GLMs or GLMMs and Kruskal-Wallis test**
1451 **in the *in vitro* SC assays.**

1452 **S1C Table. Statistical analysis outcomes from GLMs or GLMMs and Kruskal-Wallis**
1453 **tests in the IgG/IgM detection assays.**

1454 **S2 Table. Risk analysis of SCRs and demographic/clinical variables across HBB**
1455 **genotypes in *ev*SCAs.** Data from *P. falciparum*-infected samples (parasitemia ≥ 0.05% or 2500
1456 parasites/µl) collected in the Nanoro Department, Burkina Faso. Statistical tests: Chi Square
1457 /Fisher exact test, Kruskal Wallis test.

1458 **S3 Table. Median SCRs (IQR) by HBB genotype measured in *iv*SCAs with flow**
1459 **cytometry.** Timepoints measured: at 25-30 hpi and 35-40 hpi (Generation 1).

1460 **S4 Table. Risk analysis of factors across HBB genotype groups, in *iv*SCAs.**

1461 **S5 Table. RBC counts per µl analyzed during flow cytometry to exclude rule hemolysis**
1462 **of fragile mutant RBCs.** Measurements were done at three timepoints: 35-40 hpi (Generation
1463 0), and 25-30 hpi and 35-40 hpi (Generation1), for HbAC; HbAS, HbSS and HbSC RBCs.
1464 Statistical test: Kruskal-Wallis.

1465 **S6 Table. Analysis of parasite stage development by individual parasite culture within**
1466 **each HBB genotype group.** Parameters (PMR, late-stage proportions, fold changes) compared
1467 to HbAA reference and color-coded. Cultures classified as expected, delayed, or (partially)
1468 arrested/extremely delayed. SCR at 35-40 hpi (Generation 1) also shown.

1469 **S7 Table. Median IgG- and IgM-positive proportions of total, asexual, and sexual iRBCs**
1470 **by HBB genotype.** Measurements done by flow cytometry.

1471 **S8 Table. Demographics of participants in IgG/IgM detection assays across HBB**
1472 **genotype groups.** Data was analyzed in *P. falciparum* infected and non-infected plasma
1473 samples collected in the Nanoro Department, Burkina Faso within the context of the *InHost*
1474 study.

1475 **S9 Table. Key resources, primers, and probe sequences.**

1476 **S10 Table. Overview of experiments and number of cryopreserved RBC samples by HBB**
1477 **genotype.**

1478